PLOS ONE

RESEARCH ARTICLE

Robust tracking control for a quadrotor subjected to disturbances using new hyperplane-based fast Terminal Sliding Mode

Moussa Labbadi[1]*, Jamshed Iqbal[2]*, Mohamed Djemai[1], Yassine Boukal[3], Yassine Bouteraa[4,5]

1 Univ. Grenoble Alpes, CNRS, Grenoble INP, GIPSA-lab, Grenoble, France, **2** School of Computer Science, Faculty of Science and Engineering, University of Hull, Hull, United Kingdom, **3** Aeronautics, Space & Defense Division, ALTRAN, Blagnac, France, **4** College of Computer Engineering and Sciences, Prince Sattam bin Abdulaziz University, Al-Kharj, Saudi Arabia, **5** Control and Energy Management Laboratory (CEM Lab.), Ecole Nationale d Ingenieurs de Sfax (ENIS) & Institut Superieur de Biotechnologie de Sfax (ISBS), University of Sfax, Sfax, Tunisia

* moussa.labbadi@gipsa-lab.grenoble-inp.fr (ML); j.iqbal@hull.ac.uk (JI)

Citation: Labbadi M, Iqbal J, Djemai M, Boukal Y, Bouteraa Y (2023) Robust tracking control for a quadrotor subjected to disturbances using new hyperplane-based fast Terminal Sliding Mode. PLoS ONE 18(4): e0283195. https://doi.org/10.1371/journal.pone.0283195

Editor: Ning Cai, Beijing University of Posts and Telecommunications, CHINA

Received: February 10, 2022

Accepted: March 4, 2023

Published: April 24, 2023

Data Availability Statement: All relevant data are within the paper.

Funding: The author(s) received no specific funding for this work.

Competing interests: The authors have declared that no competing interests exist.

Abstract

This paper presents a finite-time approach for tracking control of a quadrotor system subjected to external disturbances and model uncertainties. The proposed approach offers a preassigned performance guarantee. Firstly, integral terminal sliding manifolds and nonsingular terminal sliding manifolds are considered to produce the new hyperplane sliding variables for both position and attitude of a quadrotor. The designed hyperplane sliding variables guaranteed a finite-time convergence. The objective is to develop a finite-time control scheme for a disturbed quadrotor to follow a predefined trajectory based on a nonlinear sliding mode controller. The main contribution of this paper is to design a hyperplane-based nonlinear sliding mode control strategy for a quadrotor subjected to disturbances. A concept of robust controllers for a quadrotor is presented based on Lyapunov theory, which proves finite-time stability of the proposed control technique. Numerical simulations with two different scenarios verify the accuracy of the proposed hyperplane-based sliding mode control approach. The simulations study also included a comparison with another nonlinear controller. Results demonstrated overperformance of the proposed control strategy.

1 Introduction

Quadrotor unmanned aerial vehicles (UAVs) have been used in a variety of applications, including precision takeoff, tactical reconnaissance, management and rescue missions, environmental protection, courier/delivery, surveillance, and reconnaissance operations; [1, 2]. The control of the quadrotor can be achieved by precisely following a particular trajectory. The quadrotor system is highly nonlinear and inherently unstable by nature [3, 4]. In addition, the highly coupled dynamics of a quadrotor makes control design more difficult. Furthermore, during indoor/outdoor flight, the quadrotor system is subject to nonlinearities from multiple

sources such as model uncertainties, external disturbances, and unmodeled dynamics, which reduces the accuracy of the quadrotor UAV tracking control.

Therefore, the design of a robust tracking controller is the key to overcoming these problems and enabling the quadrotor to track a predefined trajectory. Adaptive backstepping was introduced by [5, 6] to improve the tracking performance of a quadrotor. The authors of [7–10] proposed a fractional order (FO) sliding mode control (SMC) technique to improve the transient performance of a quadrotor system. The authors of [11] proposed the self-triggered SMC for a quadrotor under disturbances. In recent years, different SMC techniques have been devoted to tracking control [12, 13]. In this paper, a finite time control is proposed for the position and attitude of a quadrotor under disturbances. There are some other nonlinear and intelligent control methods like fuzzy logic control [14], which uses min-max rules that are not robust and pose difficulties in proving its analytical stability. Similarly, backstepping can be used to track the desired trajectory of a quadrotor, however, convergence in finite time is not assured by this control method.

In terms of ease of implementation and robustness against uncertainties and external disturbances, the SMC is a potent tool for complex nonlinear systems. In our previous work [15], we used a nonlinear manifold with non-singular terminal sliding mode (NTSM) for a quadrotor. The disadvantage of the SMC is the occurrence of chattering in system inputs [16]. Several solutions have been proposed in the literature to resolve this chattering problem, including the super twisting integral SMC [17], high-order SMC [18], and the finite-time control methods including, fast terminal SMC (FTSMC) algorithms [12]. The TSMC's biggest flaw is its one-of-a-kind problem. A new continuous integral of the sign of the error is proposed in [19] to address this problem while maintaining robustness. Also used was a decent variety of the terminal SMC (TSMC) method known as nonsingular TSMC (NTSMC) [15]. As a result of integrating the benefits of ITSMC and NTSMC, this research proposes a new hyperplane sliding mode technique for quadrotor systems subjected to external disturbances.

In [20], an improved integral of signum error control technique is investigated for the robust tracker design of quadrotor system under disturbances. In [21], the super-twisting algorithm and adaptive dynamic programming techniques have been combined for the tracking control problem of quadrotor subjected to complex disturbances. In order to estimate the external disturbances, an adaptive TSM disturbance observer is proposed. The work presented in [22] combined adaptive super twisting and nonsingular TSMC for quadrotor in the presence of bounded disturbances. Online control laws are designed to estimate exactly the upper bound of disturbances. The authors of [13] proposed a novel FO fast integral TSMC technique for position/attitude of a quadrotor to enhance the tracking performance against external disturbances. To achieve a finite-time tracking control of a quadrotor under actuators, disturbances, and input saturation, the authors in [23] proposed a neural network based on a fault tolerance control approach. The authors of [24] proposed a fixed-time convergence and disturbance rejection control approaches for a quadrotor attitude. The work developed in [25] combined a fixed nonsingular TSMC and observer for a robust control tracking of uncertain quadrotor under uncertainties. In order to stabilize an uncertain quadrotor and to make it to track a predefined flight trajectory, two PD control techniques, and adaptive fuzzy TSMC are proposed in [26]. In [27], a new observer-based control approach is proposed for controlling a quadrotor under disturbances and noisy measurements. The authors of [28] investigated to present new finite-time control and fixed time prescribed performance for a quadrotor system. In order to reduce the chattering problem, the paper [29] presented an aperiodic signal updating for a quadrotor under external disturbances and uncertainties. The authors of [30] proposed an adaptive finite-time control for a quadrotor using backstepping and global sliding mode controllers. In [31], barrier function and nonsingular terminal SMC are proposed for a

quadrotor. Event-triggered fractional-order SMC approach was proposed for UAV under disturbances. In [32], a conditional integrator SMC was developed for a quadrotor. An observer based rotor failure compensation for a quadrotor was proposed in [33]. In [34], a hybrid controller based on backstepping and integral SMC was proposed for a quadrotor. In [35], an observer-based backstepping control was proposed for a uas.

In this paper, a robust integral non-singular hyperplane SMC (INH-SMC) scheme is designed to control the disturbed quadrotor and ensures accurate tracking under the effect of disturbances. For the attitude and position subsystems, novel integral-type hyperplane-based sliding manifolds are designed. The proposed manifolds for quadrotor system are designed by combining integral-type TSMC and nonsingular TSMC to obtain robust, accurate tracking performance, and fast convergence of the state variables. The result input signals are integrated to achieve continuous controllers, which reduces the chattering phenomenon. The proposed control scheme addressed and rejected the disturbances. Contributions of this research paper can be highlighted as follows:

- Integral-type sliding and nonsingular terminal sliding manifolds are combined and applied to attitude and position of a quadrotor, which offers high tracking accuracy and faster convergence, reduces the steady-state error, and demonstrates stronger robustness against disturbances.
- Switching laws are proposed to deal with the upper bound of the disturbances that affects the dynamics.
- The proposed control scheme is applied to quadrotor dynamics in the presence of disturbances and confirmed its superiority compared to super twisting algorithms by simulation results.

The rest parts of the present paper are structured as follows. The formulation problem is given in Section II. The proposed control scheme and its stability are presented in Section III. The results are provided in Section IV. Finally, conclusions are presented in Section V.

2 Model of flight dynamics

In this section, a modeling system of a quadrotor is presented. As depicted in Fig 1, two frames are defined: an inertial reference frame $E = \{O_e, X_e, Y_e, Z_e\}$ and a body-fixed frame $B = \{O_b, X_b, Y_b, Z_b\}$.

Let's define the Euler angles related to an inertial frame and the angle velocities respectively by $\mathcal{X}_\omega(t) = [\phi(t),\ \theta(t),\ \psi(t)]^T$ and $\dot{\mathcal{X}}_\omega(t) = [\dot{\phi}(t),\ \dot{\theta}(t),\ \dot{\psi}(t)]^T$. The linear velocity can be defined $\mathcal{V}(t) = [p(t),\ q(t),\ r(t)]^T$. Let's introduce the position and linear velocity in the earth-frame respectively by $\mathcal{X}_\Upsilon(t) = [x(t),\ y(t),\ z(t)]^T$ and $\mathcal{V} = [u(t),\ v(t),\ w(t)]^T$. In order to obtain the dynamic model of the quadrotor, following assumptions are considered as in [15]:

Assumption 1. *The construction of quadrotor is symmetrical and rigid.*

Assumption 2. *The yaw, roll/pitch angles are limited respectively by* $\left(-\frac{\pi}{2}, \frac{\pi}{2}\right)$ *and* $(-\pi, \pi)$.

Using the Newton-Euler laws, the quadrotor model can be presented in the following equation.

$$\dot{\mathcal{X}}_\Upsilon(t) = \mathcal{V}(t) \tag{1a}$$

$$\omega(t) = \mathcal{R}_q \mathcal{X}_\omega(t) \tag{1b}$$

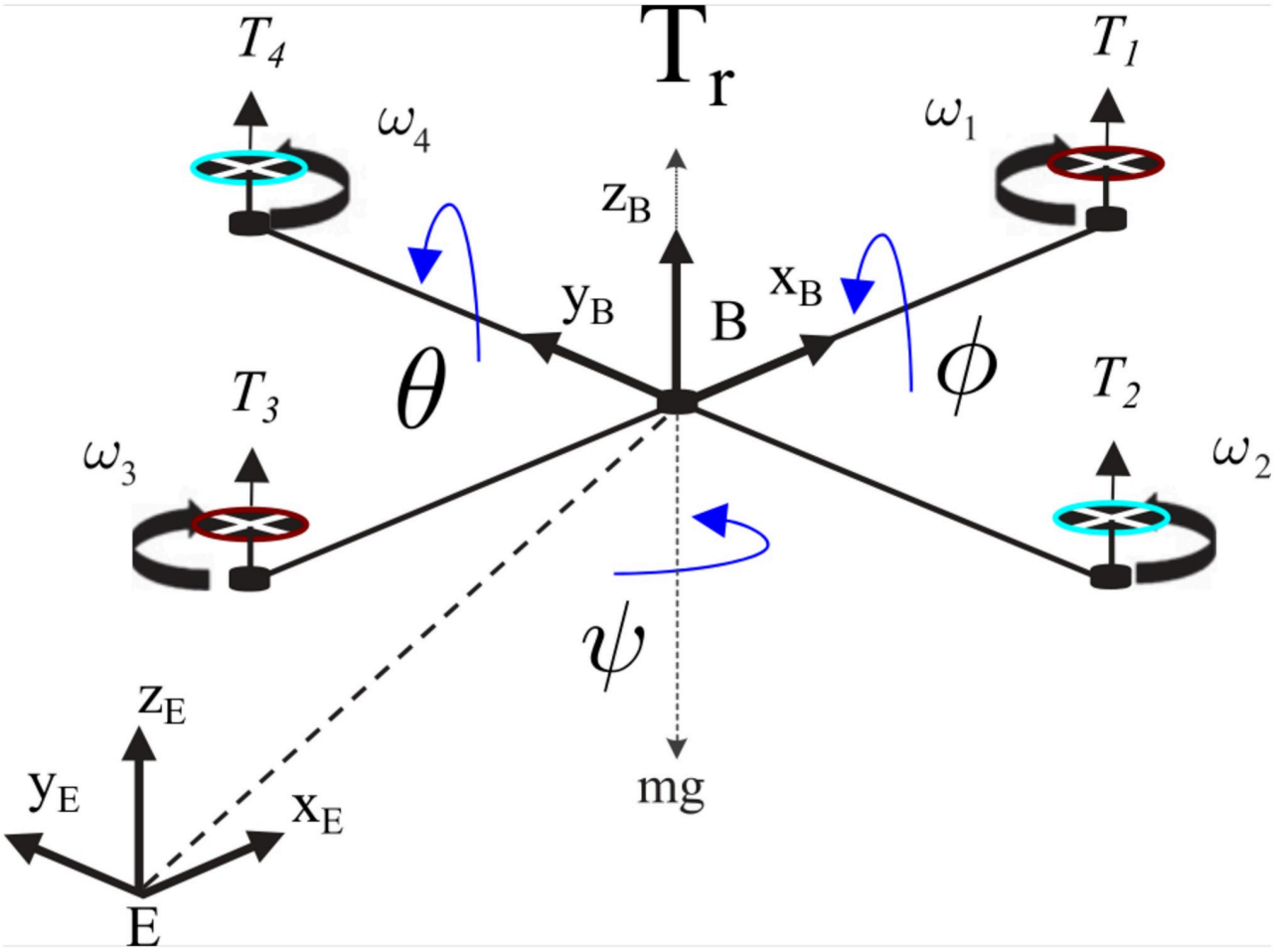

Fig 1. Quadrotor configuration.

https://doi.org/10.1371/journal.pone.0283195.g001

$$I\omega(t) = -\omega(t) \times (I\omega(t)) + \mathcal{L}_{res}, \tag{1c}$$

in which, $I = diag(I_x,\ I_y,\ I_z) \in \mathbb{R}^{3x3}$ is a symmetric positive matrix that represents the inertia of the quadrotor axes. The notation $\mathcal{R}_q$ is the rotation velocities matrix which is given as:

$$\mathcal{R}_q = \begin{bmatrix} 1 & 0 & -\sin(\theta(t)) \\ 0 & \sin(\phi(t)) & \cos(\theta(t))\sin(\phi(t)) \\ 0 & -\sin(\phi(t)) & \cos(\theta(t))\cos(\phi(t)) \end{bmatrix} \tag{2}$$

$\mathcal{L}_{res}$ is the contributed moment torque in the quadrotor center, which is written as:

$$\mathcal{L}_{res} = \mathcal{L} - \mathcal{L}_G - \mathcal{L}_D \tag{3}$$

where $\mathcal{L}$ is the torque provided by four rotors quadrotor.

$$\mathcal{L} = \begin{bmatrix} u_2 \\ u_3 \\ u_4 \end{bmatrix} = \begin{bmatrix} 0 & -\rho_y d & 0 & -\rho_y d \\ -\rho_y d & 0 & \rho_y d & 0 \\ -\rho_z & \rho_z & -\rho_z & \rho_z \end{bmatrix} \begin{bmatrix} \omega_1^2 \\ \omega_2^2 \\ \omega_3^2 \\ \omega_4^2 \end{bmatrix} \tag{4}$$

with u_2, u_3, u_4 denote the quadrotor torques. ρ_y is a positive value representing the lift constant, d represents the distance between the quadrotor mass center and rotor, and ρ_z is the drag factor.

The gyroscopic effect can be expressed as $\mathcal{L}_G = \sum_{i=1}^{4} J_r(\omega \times e_3)(-1)^{+1} + \omega_i$, in which j_r denotes the inertia of the rotor blade, ω is the rotor speed, and $e_3 = [0, 0, 1]^T$. The $\mathcal{L}_D$ is recognized as aerodynamic friction torques which is defined as $\mathcal{L}_D = diag(K_1,\ K_2,\ K_3)$, while K_1, K_2, K_3 are positive aerodynamic drag coefficients. The mathematical model of the QUAV in the presence of disturbances can be presented as follows:

$$\begin{aligned}
\ddot{\phi}(t) &= \mathcal{M}_1\dot{\theta}(t)\dot{\psi}(t) + \mathcal{M}_2\dot{\theta}(t) + \mathcal{M}_3\dot{\phi}^2(t) + \mathcal{N}_1 u_4 + \mathcal{D}_\phi(t) \\
\ddot{\theta}(t) &= \mathcal{M}_4\dot{\phi}(t)\dot{\psi}(t) + \mathcal{M}_5\dot{\phi}(t) + \mathcal{M}_6\dot{\theta}^2(t) + \mathcal{N}_2 u_3 + \mathcal{D}_\theta(t) \\
\ddot{\psi}(t) &= \mathcal{M}_7\dot{\phi}(t)\dot{\theta}(t) + \mathcal{M}_8\dot{\psi}^2(t) + \mathcal{N}_3 u_4 + \mathcal{D}_\psi(t) \\
\ddot{x}(t) &= \mathcal{M}_9\dot{x}(t) + \frac{1}{m}(\cos\phi(t)\sin\theta(t)\cos\psi(t) + \sin\phi(t)\sin\psi(t))u_1 + \mathcal{D}_x(t) \\
\ddot{y}(t) &= \mathcal{M}_{10}\dot{y(t)} + \frac{1}{m}(\cos\phi(t)\sin\theta(t)\sin\psi(t) - \sin\phi(t)\cos\psi(t))u_1 + \mathcal{D}_y(t) \\
\ddot{z}(t) &= \mathcal{M}_{11}\dot{z}(t) - g + \frac{1}{m}(\cos\phi(t)\cos\theta(t))u_1 + \mathcal{D}_z(t)
\end{aligned} \tag{5}$$

with: $\mathcal{M}_1 = \frac{(I_y - I_z)}{I_x}$, $\mathcal{M}_2 = \frac{-\omega_r J_r}{I_x}$, $\mathcal{M}_3 = \frac{-K_1}{I_x}$, $\mathcal{M}_4 = \frac{(I_z - I_x)}{I_y}$, $\mathcal{M}_5 = \frac{\omega_r J_r}{I_y}$, $\mathcal{M}_6 = \frac{-K_2}{I_y}$, $\mathcal{M}_7 = \frac{(I_x - I_y)}{I_z}$, $\mathcal{M}_8 = \frac{-K_3}{I_z}$, $\mathcal{M}_9 = \frac{-K_5}{m}$, $\mathcal{M}_{10} = \frac{-K_4}{m}$, $\mathcal{M}_{11} = -\frac{K_6}{m}$, $\mathcal{N}_1 = \frac{d}{I_x}$, $\mathcal{N}_2 = \frac{d}{I_y}$, $\mathcal{N}_3 = \frac{1}{I_z}$ and $\omega_r = \omega_1 - \omega_2 + \omega_3 - \omega_4$. $\mathcal{D}_i(t) = [\mathcal{D}_x(t), \mathcal{D}_y(t), \mathcal{D}_z(t), \mathcal{D}_\theta(t), \mathcal{D}_\theta(t), \mathcal{D}_\psi(t)]^T$ is time-varying bounded disturbance. The underactuated problem is solved by creating the following virtual control inputs.

$$v = \begin{bmatrix} v_x \\ v_y \\ v_z \end{bmatrix} = \begin{bmatrix} (\cos\phi(t)\sin\theta(t)\cos\psi(t) + \sin\phi(t)\sin\psi(t))\frac{u_1}{m} \\ (\cos\phi(t)\sin\theta(t)\sin\psi(t) - \sin\phi(t)\cos\psi(t))\frac{u_1}{m} \\ \left(-g + \frac{1}{m}\left(\cos\phi(t)\cos\theta(t)\frac{u_1}{m}\right)\right. \end{bmatrix} \tag{6}$$

According Eq (6), the total lift and tilting angles can be defined as follows:

$$\phi^{des}(t) = \arctan\left(\cos\theta^{des}(t)\frac{\sin\psi^{des}(t)v_x - \cos\psi^{des}(t)v_y}{v_z + g}\right) \tag{7a}$$

$$\theta^{des}(t) = \arctan\left(\frac{\cos\psi^{des}(t)v_x + \sin\psi^{des}(t)v_y}{v_z + g}\right) \tag{7b}$$

$$u_1 = m\sqrt{v_x^2 + v_y^2 + (v_z + g)^2} \tag{7c}$$

Assumption 3. *In this paper, the perturbation applied for each subsystem of the quadrotor, is bounded but unknown and satisfies* $|\mathcal{D}_i(t)| \leq d_i$, *where* $d_i > 0$.

3 Finite-time control design for a quadrotor using a new hyperplane based on integral non-singular SMC

In this section, a new control scheme is proposed for finite-time tracking control quadrotor system in the presence of external disturbances. Fig 2 shows the structure block of the proposed finite-time control for a quadrotor system. This finite-time control method is applied in the outer-loop control, which is realized by changing the attitude angles in the inner loop of a quadrotor. The outer-loop is used to generate the desired angles and the total thrust. The inner-loop is used to generate the rolling, pitching, and yawing torques. Two sliding mode variables are suggested for a quadrotor system, the first is an integral terminal sliding mode surface and the second is nonsingular TSMS. Based on these sliding manifolds, a new hyperplane-based sliding manifolds are developed for position/attitude subsystems. Then, the Lyapunov theory is used to prove the stability of the proposed controller.

3.1 New hyperplane-based sliding manifolds for a quadrotor position

A hyperplane-based sliding manifold is constructed using the integral terminal sliding mode (ITSM) [36] and the nonsingular terminal sliding mode (NTSM) [37] to achieve easy, precise, and robust tracking control for a quadrotor position.

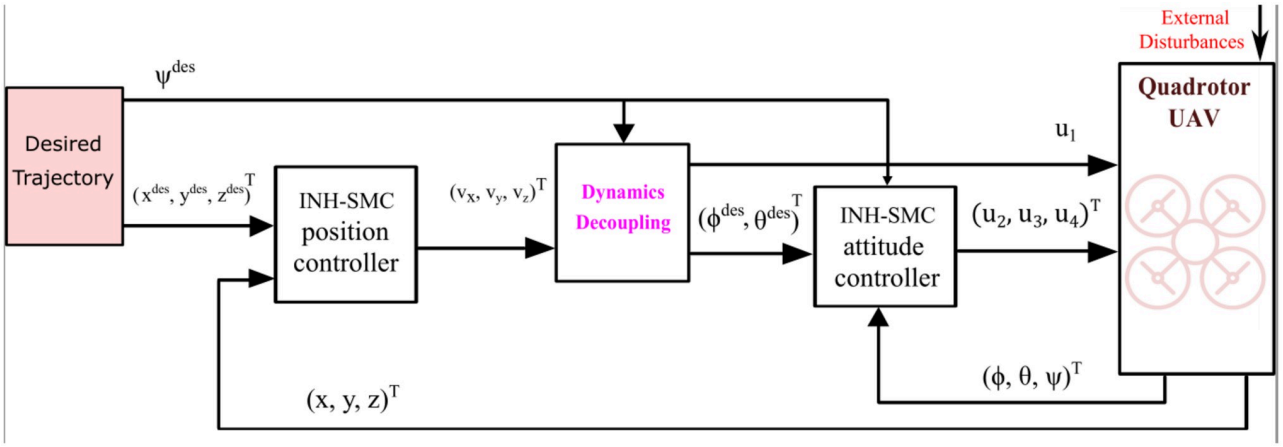

Fig 2. Structure block of the proposed control scheme.

https://doi.org/10.1371/journal.pone.0283195.g002

Define the tracking errors of position as:

$$e_7(t) = x(t) - x^{des}(t), \quad e_9(t) = y(t) - y^{des}(t), \quad e_{11}(t) = z(t) - z^{des}(t) \tag{8}$$

The integral terminal sliding mode variable for the position can be described in order to ensure robustness and minimize steady state-errors as:

$$\begin{cases} \sigma_7(t) & = \Xi_{x1} e_7(t) + \Xi_{x2} \int |e_7(t)|^{\mu_x} sign(e_7(t)) dt \\ \sigma_9(t) & = \Xi_{y1} e_9(t) + \Xi_{y2} \int |e_9(t)|^{\mu_y} sign(e_9(t)) dt \\ \sigma_{11}(t) & = \Xi_{z1} e_{11}(t) + \Xi_{z2} \int |e_{11}(t)|^{\mu_z} sign(e_{11}(t)) dt \end{cases} \tag{9}$$

where Ξ_{i1} and Ξ_{i2} for $i = x, y, z$ are positive parameters and $\frac{1}{2} < \mu_i < 1$.

In order to achieve fast convergence and high tracking, hyperplane based sliding manifolds are designed using NTSM as follows:

$$s_7(t) = \sigma_7(t) + \frac{1}{\beta_x} \dot{\sigma}_7^{\gamma_x}(t), \quad s_9(t) = \sigma_9(t) + \frac{1}{\beta_y} \dot{\sigma}_9^{\gamma_y}(t), s_{11}(t) = \sigma_{11}(t) + \frac{1}{\beta_z} \dot{\sigma}_{11}^{\gamma_z}(t) \tag{10}$$

in which, $\beta_{x,y,z}$ is positive coefficient, and $1 < \gamma_{x,y,z} < 2$. The designed hyperplane-based sliding manifold for position of a quadrotor is suggested to force $s_{7,9,11}(t)$ converge to zero for any conditions of $\sigma_{7,9,11}(t)$.

3.2 Finite-time control design for position loop

The controller introduced in this paper is composed of two control laws: one is a continuous control law, while the other is a discontinuous control law.

3.2.1 Continuous control law for position loop. This component can be obtained by setting $\dot{s}_{7,9,11}(t) = 0$ in without disturbances $\mathcal{D}_{7,9,11}(t) = 0$.

The time derivative of σ_i can be given by:

$$\begin{aligned} \dot{s}_{7,9,11}(t) & = \dot{\sigma}_{7,9,11}(t) + \frac{\gamma_{7,9,11}}{\beta_{7,9,11}} \dot{\sigma}_{7,9,11}^{\gamma_{7,9,11}-1}(t) \ddot{\sigma}_{7,9,11}(t) \\ & = \frac{\gamma_{7,9,11}}{\beta_{7,9,11}} \dot{\sigma}_{7,9,11}^{\gamma_{7,9,11}-1}(t) \left(\frac{\beta_{7,9,11}}{\gamma_{7,9,11}} \dot{\sigma}_i^{2-\gamma_{7,9,11}}(t) + \ddot{\sigma}_{7,9,11}(t)\right) \end{aligned} \tag{11}$$

The time derivative of $\sigma_{7,9,11}(t)$ and its double time derivative are respectively given as:

$$\dot{\sigma}_{7,9,11}(t) = \Xi_{i1} \dot{e}_{7,9,11}(t) + \Xi_{i2} |e_{7,9,11}|^{\mu_i}(t) sign(e_{7,9,11}(t)) \tag{12}$$

and

$$\ddot{\sigma}_{7,9,11}(t) = \Xi_{i1} \ddot{e}_{7,9,11}(t) + \Xi_{i2} \mu_i |e_{7,9,11}|^{\mu_i - 1}(t) \dot{e}_{7,9,11}(t) \tag{13}$$

By assuming that (10) is equal to zero, one get:

$$\dot{e}_{7,9,11}(t) = -\frac{\Xi_{i1}}{\Xi_{i2}} |e_{7,9,11}|^{\mu_i}(t) sign(e_{7,9,11}(t)) \tag{14}$$

Submitting (14) in (12), the double time derivative of s_i is given by the following equation.

$$\ddot{\sigma}_{7,9,11}(t) = \Xi_{i1} \ddot{e}_{7,9,11}(t) - \frac{\mu_i \Xi_{i2}^2}{\Xi_{i1}} |e_{7,9,11}|^{2\mu_i - 1}(t) sign(e_{7,9,11}(t)) \tag{15}$$

Submitting (15) in (11), it produces that

$$\begin{aligned}\dot{s}_{7,9,11}(t) = \frac{\gamma_i}{\beta_i}\dot{\sigma}_{7,9,11}^{\gamma_i-1}(t)(\frac{\beta_i}{\gamma_i}\dot{\sigma}_{7,9,11}^{2-\gamma_i}(t) + \Xi_{i1}\ddot{e}_{7,9,11}(t) \\ - \frac{\mu_i\Xi_{i2}^2}{\Xi_{i1}}|e_{7,9,11}(t)|^{2\mu_i-1}sign(e_{7,9,11}(t)))\end{aligned} \tag{16}$$

By setting $\dot{s}_{7,9,11}(t) = 0$ and tacking $\mathcal{D}_{7,9,11}(t) = 0$, the equivalent rule can be obtained. Then, using the double time derivative of the tracking errors, the continuous control laws for the position of a quadrotor are given by:

$$\begin{aligned} v_{xc} &= \frac{1}{\Xi_{x1}}\left(\frac{\mu_x\Xi_x^2}{\Xi_{x1}}|e_7(t)|^{2\mu_x-1}sign(e_7(t)) - \frac{\beta_x}{\gamma_x}\dot{s}_x^{2-\gamma_x} - \Xi_{x1}\mathcal{M}_9\dot{x}(t)\right) \\ v_{yc} &= \frac{1}{\Xi_{y1}}\left(\frac{\mu_y\Xi_y^2}{\Xi_{y1}}|e_9(t)|^{2\mu_y-1}sign(e_9(t)) - \frac{\beta_y}{\gamma_y}\dot{s}_y^{2-\gamma_y} - \Xi_{y1}\mathcal{M}_{10}\dot{y}(t)\right) \\ v_{zc} &= \frac{1}{\Xi_{z1}}\left(\frac{\mu_z\Xi_z^2}{\Xi_{z1}}|e_{11}(t)|^{2\mu_z-1}sign(e_{11}(t)) - \frac{\beta_z}{\gamma_z}\dot{s}_z^{2-\gamma_z} - \Xi_{z1}\mathcal{M}_{11}\dot{z}(t) + g\right)\end{aligned} \tag{17}$$

3.2.2 Reaching control law for position loop. A switching law is added to the equivalent law to increase efficiency against model uncertainty/external disruption of a quadrotor device. Then its expressions can be given as follows:

$$\begin{aligned} v_{xs} &= \frac{1}{\Xi_{x1}}(-k_{x1}s_7(t) - k_{x2}sign(s_7(t))) \\ v_{ys} &= \frac{1}{\Xi_{y1}}\left(-k_{y1}s_9(t) - k_{y2}sign(s_9(t))\right) \\ v_{zs} &= \frac{1}{\Xi_{z1}}(-k_{z1}s_{11}(t) - k_{z2}sign(s_{11}(t)))\end{aligned} \tag{18}$$

where k_{i1} and k_{i2} for $i = 7, 9, 11$ are positive constants.

Theorem 1. *Consider the quadrotor position system* (5) *and the hyperplane-based sliding surfaces are designed in* (10) *and the control laws are designed in* (19), *then the tracking errors* (8) *of the closed-loop system can asymptotically converge to zero*.

$$\begin{aligned} v_x &= \frac{1}{\Xi_{x1}}\left(\begin{array}{c}\frac{\mu_x\Xi_x^2}{\Xi_{x1}}|e_7(t)|^{2\mu_x-1}sign(e_7(t)) - \frac{\beta_x}{\gamma_x}\dot{s}_x^{2-\gamma_x} - \Xi_{x1}\mathcal{M}_9\dot{x}(t) - k_{x1}s_7(t) \\ - k_{x2}sign(s_7(t))\end{array}\right) \\ v_y &= \frac{1}{\Xi_{y1}}\left(\begin{array}{c}\frac{\mu_y\Xi_y^2}{\Xi_{y1}}|e_9(t)|^{2\mu_y-1}sign(e_9(t)) - \frac{\beta_y}{\gamma_y}\dot{s}_y^{2-\gamma_y} - \Xi_{y1}\mathcal{M}_{10}\dot{y}(t) - k_{y1}s_9(t) \\ - k_{y2}sign(s_9(t))\end{array}\right) \\ v_z &= \frac{1}{\Xi_{z1}}\left(\begin{array}{c}\frac{\mu_z\Xi_z^2}{\Xi_{z1}}|e_{11}(t)|^{2\mu_z-1}sign(e_{11}(t)) - \frac{\beta_z}{\gamma_z}\dot{s}_z^{2-\gamma_z} - \Xi_{z1}\mathcal{M}_{11}\dot{z}(t) + g \\ - k_{z1}s_{11}(t) - k_{z2}sign(s_{11}(t))\end{array}\right)\end{aligned} \tag{19}$$

Proof. Define a Lyapunov function for the position and attitude of a quadrotor in terms of $s_7(t)$, $s_9(t)$, and $s_{11}(t)$ as:

$$V_1 = 0.5[s_7^2(t) + s_9^2(t) + s_{11}^2(t)] \tag{20}$$

Differentiating V_Σ, it yields

$$\dot{V}_1 = s_7(t)\dot{s}_7(t) + s_9(t)\dot{s}_9(t) + s_{11}(t)\dot{s}_{11}(t) \tag{21}$$

Now, by using (16) and (19),

$$\begin{aligned}\dot{V}_1 = {} & s_7(t)\frac{\gamma_x}{\beta_x}\dot{s}_7^{\gamma_x-1}(t)[\Xi_{x1}\mathcal{D}_x(t) - k_{x1}s_7(t) - k_{x2}sign(s_7(t))] \\ & + s_9(t)\frac{\gamma_y}{\beta_y}\dot{s}_9^{\gamma_y-1}(t)[\Xi_{y1}\mathcal{D}_y(t) - k_{y1}s_9(t) - k_{y2}sign(s_9(t))] \\ & + s_{11}(t)\frac{\gamma_z}{\beta_z}\dot{s}_{11}^{\gamma_z-1}(t)[\Xi_{z1}\mathcal{D}_z(t) - k_{z1}s_{11}(t) - k_{z2}sign(s_{11}(t))]\end{aligned} \tag{22}$$

Using (11), the above equation leads to

$$\begin{aligned}\dot{V}_1 \leq {} & -\frac{\gamma_x}{\beta_x}\dot{s}_7^{\gamma_x-1}(t)k_{x1}s_7^2(t) - \frac{\gamma_y}{\beta_y}\dot{s}_9^{\gamma_y-1}(t)k_{y1}s_9^2(t) - \frac{\gamma_z}{\beta_z}\dot{s}_{11}^{\gamma_z-1}(t)k_{z1}s_{11}^2(t) \\ & \leq 0\end{aligned} \tag{23}$$

For any initial state $s_{7,9,11}(t) \neq 0$, define t_{ri} the reaching time to converge to zero. After that, $\sigma_{7,9,11}(t)$ will converge to zero as a consequence. The total time t_{fi} can be written as follows [37, 38]

$$t_{fi} = t_{ri} + \frac{\gamma_i}{\gamma_i - 1}\beta_i^{-\frac{1}{\gamma_i}}|\sigma(t_{ri})|^{\frac{\gamma_i - 1}{\gamma_i}} \tag{24}$$

As a result, the position tracking errors will asymptotically converge to zero.

The suggested controller is used for the position subsystem in this subsection, and the Lyapunov principle is used to prove the loop's stability. In the next section, we'll use the same steps we used for the position-loop to produce control torques, which stabilize the attitude-loop under disturbances.

3.3 Finite-time control design for attitude loop

By extracting the desired roll and pitch from the position control presented in the previous subsection, the torques of the quadrotor attitude can be designed in this section. Define the desired tracking errors of a quadrotor attitude as follows:

$$e_1(t) = \phi(t) - \phi^{des}(t), \quad e_3(t) = \theta(t) - \theta^{des}(t), \quad e_5(t) = \psi(t) - \psi^{des}(t) \tag{25}$$

The ITSM for the attitude can be described in order to ensure robustness and minimize steady

state-errors as:

$$\begin{cases} \sigma_1(t) & = \Xi_{\phi 1} e_1(t) + \Xi_{\phi 2} \int |e_1(t)|^{\mu_\phi} sign(e_1(t)) dt \\ \sigma_3(t) & = \Xi_{\theta 1} e_3(t) + \Xi_{\theta 2} \int |e_3(t)|^{\mu_\theta} sign(e_3(t)) dt \\ \sigma_5(t) & = \Xi_{\psi 1} e_5(t) + \Xi_{\psi 2} \int |e_5(t)|^{\mu_\psi} sign(e_5(t)) dt \end{cases} \tag{26}$$

where Ξ_{i1} and Ξ_{i2} for $i = \phi, \theta, \psi$ are positive parameters and $\frac{1}{2} < \mu_i < 1$.

In order to achieve fast convergence and high tracking, hyperplane based sliding manifolds are designed using NTSM as follows:

$$s_1(t) = \sigma_1(t) + \frac{1}{\beta_\phi} \dot{\sigma}_1^{\gamma_\phi}(t), \quad s_3(t) = \sigma_3(t) + \frac{1}{\beta_\theta} \dot{\sigma}_3^{\gamma_\theta}(t), s_5(t) = \sigma_5(t) + \frac{1}{\beta_\psi} \dot{\sigma}_5^{\gamma_\psi}(t) \tag{27}$$

in which, $\beta_{\phi,\theta,\psi}$ is positive coefficient, and $1 < \gamma_{\phi,\theta,\psi} < 2$.

Theorem 2. *Consider the quadrotor attitude system* (5) *and the hyperplane-based sliding surfaces are designed in* (27) *and the control laws are designed in* (28), *then the tracking errors* (25) *of the closed-loop system can asymptotically converge to zero*.

$$\begin{aligned} u_2 &= \frac{1}{\mathcal{N}_1 \Xi_{\phi 1}} \left(\begin{array}{l} \frac{\mu_\phi \Xi_\phi^2}{\Xi_{\phi 1}} |e_1(t)|^{2\mu_\phi - 1} sign(e_1(t)) - \frac{\beta_\phi}{\gamma_\phi} \dot{\sigma}_1^{2-\gamma_\phi}(t) - \Xi_{\phi 1} \{ \mathcal{M}_1 \dot{\theta}(t) \dot{\psi}(t) \\ \quad + \mathcal{M}_2 \dot{\theta}(t) + \mathcal{M}_3 \dot{\phi}^2(t) \} + \ddot{\phi}^{des}(t) - k_{\phi 1} s_1(t) - k_{\phi 2} sign(s_1(t)) \} \end{array} \right) \\ u_3 &= \frac{1}{\mathcal{N}_2 \Xi_{\theta 1}} \left(\begin{array}{l} \frac{\mu_\theta \Xi_\theta^2}{\Xi_{\theta 1}} |e_3(t)|^{2\mu_\theta - 1} sign(e_3(t)) - \frac{\beta_\theta}{\gamma_\theta} \dot{\sigma}_3^{2-\gamma_\theta}(t) + \Xi_{\theta 1} \{ \mathcal{M}_4 \dot{\phi}(t) \dot{\psi}(t) \\ \quad + \mathcal{M}_5 \dot{\phi}(t) + \mathcal{M}_6 \dot{\theta}^2(t) + \ddot{\theta}^{des}(t) - k_{\theta 1} s_3(t) - k_{\theta 2} sign(s_3(t)) \} \end{array} \right) \\ u_4 &= \frac{1}{\mathcal{N}_3 \Xi_{\psi 1}} \left(\begin{array}{l} \frac{\mu_\psi \Xi_\psi^2}{\Xi_{\psi 1}} |e_5(t)|^{2\mu_\psi - 1} sign(e_5(t)) - \frac{\beta_\psi}{\gamma_\psi} \dot{\sigma}_5^{2-\gamma_\psi}(t) + \Xi_{\psi 1} \{ \mathcal{M}_7 \dot{\phi}(t) \dot{\theta}(t) \\ \quad + \mathcal{M}_8 \dot{\psi}^2(t) + \ddot{\psi}^{des}(t) - k_{\psi 1} s_5(t) - k_{\psi 2} sign(s_5(t)) \} \end{array} \right) \end{aligned} \tag{28}$$

Proof. Define a Lyapunov function for the position and attitude of a quadrotor in terms of $s_1(t)$, $s_3(t)$, and $s_5(t)$ as:

$$V_2 = 0.5[s_1^2(t) + s_3^2(t) + s_5^2(t)] \tag{29}$$

Differentiating V_2, it yields

$$\dot{V}_2 = s_1(t)\dot{s}_1(t) + s_3(t)\dot{s}_3(t) + s_5(t)\dot{s}_5(t) \tag{30}$$

Now, by using the time derivative of sliding mode variables and (28),

$$\begin{aligned} \dot{V}_1 = \quad & s_1(t) \frac{\gamma_\phi}{\beta_\phi} \dot{s}_1^{\gamma_\phi - 1}(t) [\Xi_{\phi 1} \mathcal{D}_\phi(t) - k_{\phi 1} s_1(t) - k_{\phi 2} sign(s_1(t))] \\ & + s_3(t) \frac{\gamma_\theta}{\beta_\theta} \dot{s}_3^{\gamma_\theta - 1}(t) [\Xi_{\theta 1} \mathcal{D}_\theta(t) - k_{\theta 1} s_3(t) - k_{\theta 2} sign(s_3(t))] \\ & + s_5(t) \frac{\gamma_\psi}{\beta_\psi} \dot{s}_5^{\gamma_\psi - 1}(t) [\Xi_{\psi 1} \mathcal{D}_\psi(t) - k_{\psi 1} s_5(t) - k_{\psi 2} sign(s_5(t))] \end{aligned} \tag{31}$$

Using the time derivative of sliding mode variables of attitude loop, the above equation leads

to

$$\begin{aligned}\dot{V}_1 \leq & -\frac{\gamma_\phi}{\beta_\phi}\dot{s}_1^{\gamma_\phi-1}(t)k_{\phi1}s_1^2(t) - \frac{\gamma_\theta}{\beta_\theta}\dot{s}_3^{\gamma_\theta-1}(t)k_{\theta1}s_3^2(t) - \frac{\gamma_\psi}{\beta_\psi}\dot{s}_5^{\gamma_\psi-1}(t)k_{\psi1}s_5^2(t) \\ & \leq 0\end{aligned} \tag{32}$$

For any initial state $s_{1,3,5}(t) \neq 0$, define t_{rj} the reaching time to converge to zero. After that, $\sigma_{1,3,5}(t)$ will converge to zero as a consequence. The total time t_{fj} can be written as follows [37, 38]

$$t_{fj} = t_{rj} + \frac{\gamma_j}{\gamma_j - 1}\beta_j^{-\frac{1}{\gamma_j}}|\sigma(t_{rj})|^{\frac{\gamma_j-1}{\gamma_j}} \tag{33}$$

As a result, the position tracking errors will asymptotically converge to zero.

3.4 Stability analysis of closed loop system

The following Theorem shows the results of the proposed controller and the stability of the closed-loop system is provided.

Theorem 3. *Consider the quadrotor system* (5) *and the hyperplane-based sliding surfaces s are designed as* (10), (27) *and the control laws are designed as* (19) and (28), *then the tracking errors* (8) *and* (25) *of the closed-loop system can asymptotically converge to zero.*

Proof. Define a Lyapunov function for the position and attitude of a quadrotor in terms of $s_7(t)$, $s_9(t)$, $s_{11}(t)$, $s_1(t)$, $s_3(t)$, and $s_5(t)$ as:

$$V_{12} = 0.5[s_7^2(t) + s_9^2(t) + s_{11}^2(t) + s_1^2(t) + s_3^2(t) + s_5^2(t)] \tag{34}$$

Differentiating V_{12}, it yields

$$\dot{V}_{12} = s_7(t)\dot{s}_7(t) + s_9(t)\dot{s}_9(t) + s_{11}(t)\dot{s}_{11}(t) + s_1(t)\dot{s}_1(t) + s_3(t)\dot{s}_3(t) + s_5(t)\dot{s}_5(t) \tag{35}$$

Now, by using the time derivative of position and attitude sliding mode variables, (19), and (28),

$$\begin{aligned}\dot{V}_{12} = & \; s_7(t)\frac{\gamma_x}{\beta_x}\dot{s}_x^{\gamma_x-1}[\Xi_{x1}\mathcal{D}_x(t) - k_{x1}s_7(t) - k_{x2}sign(s_7(t))] \\ & + s_9(t)\frac{\gamma_y}{\beta_y}\dot{s}_y^{\gamma_y-1}[\Xi_{y1}\mathcal{D}_y(t) - k_{y1}s_9(t) - k_{y2}sign(s_9(t))] \\ & + s_{11}(t)\frac{\gamma_z}{\beta_z}\dot{s}_z^{\gamma_z-1}[\Xi_{z1}\mathcal{D}_z(t) - k_{z1}s_{11}(t) - k_{z2}sign(s_{11}(t))] \\ & + s_1(t)\frac{\gamma_\phi}{\beta_\phi}\dot{s}_\phi^{\gamma_\phi-1}[\Xi_{\phi1}\mathcal{D}_\phi - k_{\phi1}s_1(t) - k_{\phi2}sign(s_1(t))] \\ & + s_3(t)\frac{\gamma_\theta}{\beta_\theta}\dot{s}_\theta^{\gamma_\theta-1}[\Xi_{\theta1}\mathcal{D}_\theta - k_{\theta1}s_3(t) - k_{\theta2}sign(s_3(t))] \\ & + s_5(t)\frac{\gamma_\psi}{\beta_\psi}\dot{s}_\psi^{\gamma_\psi-1}[\Xi_{\psi1}\mathcal{D}_\psi - k_{\psi1}s_5(t) - k_{\psi2}sign(s_5(t))]\end{aligned} \tag{36}$$

Using (23) and (32), the above equation leads to

$$\begin{aligned}\dot{V}_{12} \leq\ & \frac{\gamma_x}{\beta_x}\dot{s}_x^{\gamma_x-1}[|s_7(t)|(\Xi_{x1}|\mathcal{D}_x(t)|-k_{x2})-k_{x1}s_7^2(t)] \\ & +\frac{\gamma_y}{\beta_y}\dot{s}_y^{\gamma_y-1}[|s_9(t)|(\Xi_{y1}|\mathcal{D}_y(t)|-k_{y2})-k_{y1}s_9^2(t)] \\ & +\frac{\gamma_z}{\beta_z}\dot{s}_z^{\gamma_z-1}[|s_{11}(t)|(\Xi_{z1}|\mathcal{D}_z(t)|-k_{z2})-k_{z1}s_{11}^2(t)] \\ & +\frac{\gamma_\phi}{\beta_\phi}\dot{s}_\phi^{\gamma_\phi-1}[|s_1(t)|(\Xi_{\phi1}|\mathcal{D}_\phi|-k_{\phi2})-k_{\phi1}s_1^2(t)] \\ & +\frac{\gamma_\theta}{\beta_\theta}\dot{s}_\theta^{\gamma_\theta-1}[|s_3(t)|(\Xi_{\theta1}|\mathcal{D}_\theta|-k_{\theta2})-k_{\theta1}s_3^2(t)] \\ & +\frac{\gamma_\psi}{\beta_\psi}\dot{s}_\psi^{\gamma_\psi-1}[|s_5(t)|(\Xi_{\psi1}|\mathcal{D}_\psi|-k_{\psi2})-k_{\psi1}s_5^2(t)]\end{aligned} \tag{37}$$

We choose $k_{x2} > \Xi_{x1}|\mathcal{D}_x(t)|$, $k_{y2} > \Xi_{y1}|\mathcal{D}_y(t)|$, $k_{z2} > \Xi_{z1}|\mathcal{D}_z(t)|$, $k_{\phi2} > \Xi_{\phi1}|\mathcal{D}_\phi|$, $k_{\theta2} > \Xi_{\theta1}|\mathcal{D}_\theta|$, and $k_{\psi2} > \Xi_{\psi1}|\mathcal{D}_\psi|$. Eq (37) becomes:

$$\begin{aligned}\dot{V}_{12} \leq\ & -\frac{\gamma_x}{\beta_x}\dot{s}_x^{\gamma_x-1}k_{x1}s_7^2(t)-\frac{\gamma_y}{\beta_y}\dot{s}_x^{\gamma_y-1}k_{y1}s_9^2(t)-\frac{\gamma_z}{\beta_z}\dot{s}_z^{\gamma_z-1}k_{z1}s_{11}^2(t) \\ & -\frac{\gamma_\phi}{\beta_\phi}\dot{s}_\phi^{\gamma_\phi-1}k_{\phi1}s_1^2(t)-\frac{\gamma_\theta}{\beta_\theta}\dot{s}_\theta^{\gamma_\theta-1}k_{\theta1}s_3^2(t)-\frac{\gamma_\psi}{\beta_\psi}\dot{s}_\psi^{\gamma_\psi-1}k_{\psi1}s_5^2(t) \\ & \leq 0\end{aligned} \tag{38}$$

Hence, the tracking errors of the position and attitude can asymptotically converge to zero. The proof is thus completed.

4 Simulation results

Numerical simulations are used to evaluate the tracking performance of the hyperplane-based sliding mode controller described in this paper. As a comparison, the super-twisting PID sliding mode controller provided in [17] is used.

4.1 Control parameters selection

During the simulation, the user has to select the value that achieves the best balance of tracking accuracy and control smoothness. The discussion of the controller parameter selection for the proposed control technique is summarized as follows:

- Selections of Ξ_{i1}, Ξ_{i2}, and μ_i for $i = x, y, z, \phi, \theta, \psi$: The parameters Ξ_{i1}, Ξ_{i2}, and μ_i are used in ITSM manifolds as given in (9) and (26). Faster convergence of the tracking errors can be obtained by choosing a smaller value of $\Xi_{i1}\Xi_{i2}$, and $\frac{1}{2} < \mu_i < 1$ For a quadrotor position and attitude loop, $\Xi_{i1} = 1$, $\Xi_{i2} = 0.0046$, and $\mu_i = 1$ are selected.
- Selections of β_i and γ_i for $i = x, y, z, \phi, \theta, \psi$: The gains β_i and γ_i are used in NTSM as shown in (10) for quadrotor position and (27) for altitude loop. Faster convergence of the tracking errors can be obtained by choosing a high positive value of β_i, and a smaller value of $1 < \gamma_i < 2$, however, it increases the magnitude of the control effort. The best choice of NTSM gains is presented in Table 2
- Selections of k_{i1} and k_{i2} for $i = x, y, z, \phi, \theta, \psi$: The positive gains k_{i1} and k_{i2} are used in the switching law (18) affect the robustness of the system by balancing the control signal smoothness. The selective values of k_{i1} and k_{i2} parameters are presented in Table 2.

Table 1. Quadrotor parameters.

Parameter	Value	Parameter	Value
$g(s^{-2}.m)$	9.8	$K_5(Nms^2)$	0.01
$m(kg)$	0.486	$K_6(Nms^2)$	0.01
$I_x(m^{-2}.kg)$	3.8278e-3	$K_1(Nrads^2)$	0.012
$I_y(m^{-2}.kg)$	3.8278e-3	$K_2(Nrads^2)$	0.012
$I_z(m^{-2}.kg)$	7.6566e-3	$K_3(Nrads^2)$	0.012
$J_r(m^{-2}.kg)$	2.8385e-5	$\rho(N.s^2)$	2.9842e-3
$K_4(Nms^2)$	0.01	$\rho_c(N.m.s^2)$	3.2320e-2

https://doi.org/10.1371/journal.pone.0283195.t001

Table 2. Control system parameters.

Parameter	Value	Parameter	Value
$\mu_{\phi,\theta,\psi}$	1	$\beta_{\phi,\theta,\psi}$	102.15
$\gamma_{\phi,\theta,\psi}$	1.9	Ξ_{i2}	0.0046
Ξ_{i1}	1	$k_{\phi 2,\theta 2,\psi 2}$	2.6997
$k_{\phi 1,\theta 1,\psi 1}$	817.6194	$k_{x1,y1,z1}$	6
$\mu_{x,y,z}$	1	$\beta_{x,y,z}$	2.1487
$\gamma_{x,y,z}$	1.1	$k_{x2,y2,z2}$	2

https://doi.org/10.1371/journal.pone.0283195.t002

Remark 1. *The design parameters of the controllers need to be tuned to achieve the satisfactory performance in terms of quadrotor trajectory-tracking in the presence of disturbances. To pick the optimal values for such parameters, the optimization toolbox in MATLAB program has been used (see Ref.* [39]).

Tables 1 and 2 list the controller and quadrotor parameters, respectively. The following are the beginning conditions for quadrotor states:

$$\begin{aligned} x_0 &= 0.05m, \quad y_0 = 1m, \quad z_0 = 0.01m, \\ \phi_0 &= 0rad, \quad \theta_0 = 0rad, \quad \psi_0 = 0rad \end{aligned} \tag{39}$$

Two scenarios in terms of disturbances path following are proposed in this section.

4.2 Simulation 1

In order to examine the tracking performance of the proposed control scheme, the complex change of the drag coefficients is considered in this scenario. This effect is shown in Figs 3 and 4, respectively for translational and rotational subsystems. The desired path used in this simulation is given by:

$$x^{des}(t) = \begin{cases} 0.5\cos(0.5t)\ m & t \in [0, 4\pi) \\ 0.5\ m & t \in [4\pi, 20) \\ 0.25t - 4.5\ m & t \in [20, 30) \\ 3\ m & t \in [30, 80] \end{cases} \quad y^{des}(t) = \begin{cases} 0.5\sin(0.5t)\ m & t \in [0, 4\pi) \\ 0.25t - 3.14\ m & t \in [4\pi, 20) \\ 5 - \pi\ m & t \in [20, 30) \\ -0.2358t + 8.94\ m & t \in [30, 40] \\ -0.5\ m & t \in [40, 80] \end{cases} \tag{40}$$

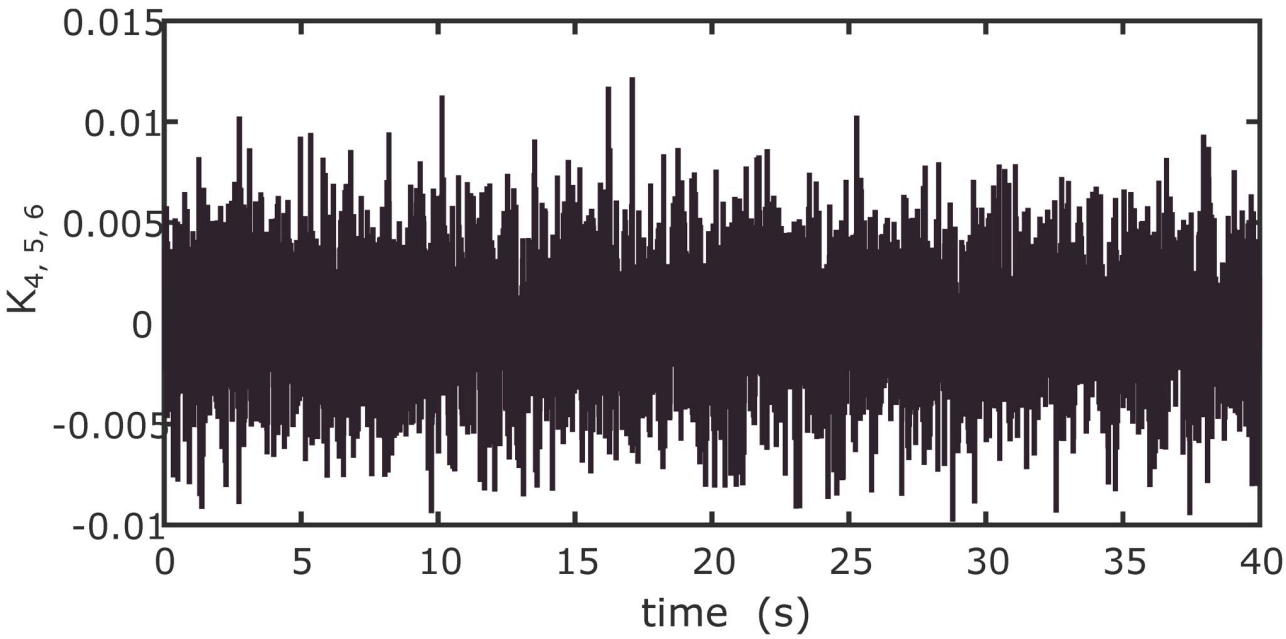

Fig 3. Drag coefficients for translational motion.

https://doi.org/10.1371/journal.pone.0283195.g003

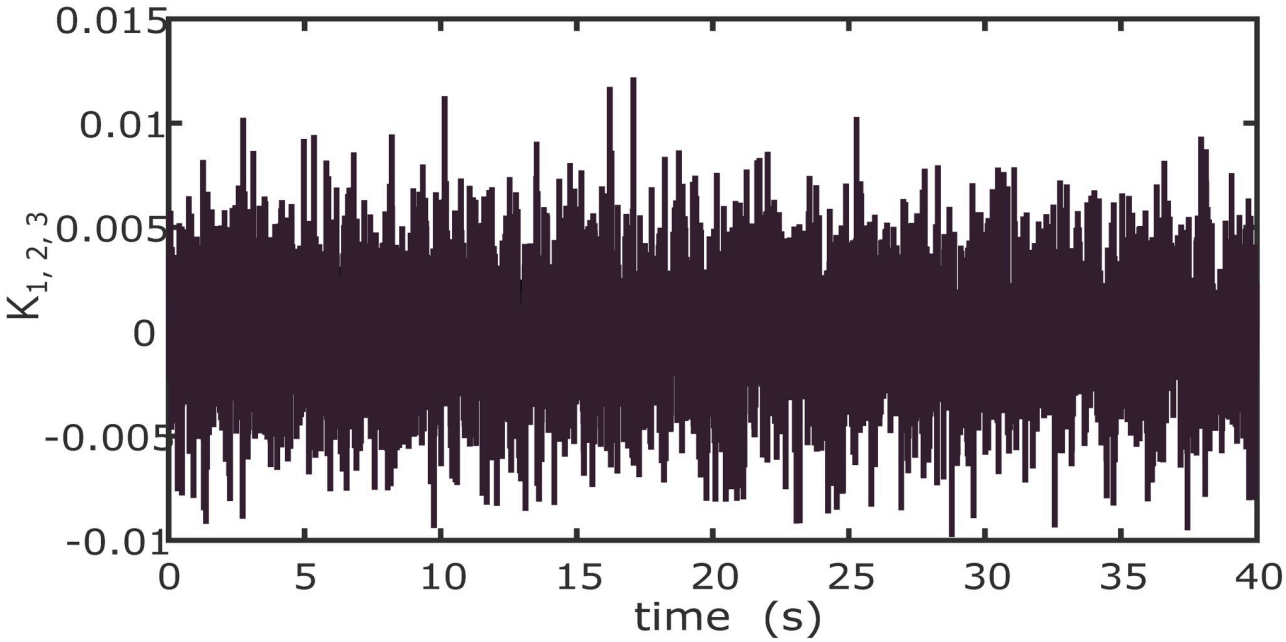

Fig 4. Drag coefficients for rotational motion.

https://doi.org/10.1371/journal.pone.0283195.g004

$$z^{des}(t) = \begin{cases} 0.125t + 1 \ m & t \in [0, 4\pi) \\ 0.5\pi + 1 \ m & t \in [4\pi, 40) \\ \exp(-0.2t + 8.944) \ m & t \in [40, 80) \end{cases} \psi^{des}(t) = \begin{cases} \frac{\pi}{4} \ rad & t \in [0, 50) \\ 0 \ rad & t \in (50, 80] \end{cases} \quad (41)$$

$$\begin{aligned} x^{des}(t) &= \sin(0.5t)m, \quad y^{des}(t) = \cos(0.5t)m, \quad z^{des}(t) = 0.1t + 2m, \\ \psi^{des}(t) &= 0.3rad \end{aligned} \quad (42)$$

External disturbances used in this simulation for quadrotor position and attitude are set as follows:

$$\begin{aligned} \mathcal{D}_x(t) &= 1 + \sin(0.2\pi t) \quad m/s^2 \\ \mathcal{D}_y(t) &= 1 + cos(0.2\pi t) \quad m/s^2 \\ \mathcal{D}_z(t) &= 0.5\cos(0.7t) + 0.7\sin(0.3) \quad m/s^2 \\ \mathcal{D}_\phi(t) &= 2\sin(0.7t) + 1 \quad rad/s^2 \\ \mathcal{D}_\theta(t) &= 2\cos(0.9t) + 1 \quad rad/s^2 \\ \mathcal{D}_\psi(t) &= 2\tanh(0.7t) \quad rad/s^2 \end{aligned} \quad (43)$$

Figs 5 to 11 demonstrate the trajectory tracking responses utilizing the control methodology suggested in this paper and a super-twisting PID sliding mode controller. The absolute position result is plotted in Fig 5; as can be seen from these results, the proposed controller ensures that the quadrotor follows the desired trajectory with great precision, even when external disturbances are present. The suggested controller produced faster position responses than the SP-PIDSMC approach, as illustrated in Fig 5. The roll, pitch, and yaw angles converge to their intended angles in a short finite time, as shown in Fig 6. The vehicle is more stable under the proposed controller under the disturbed flight. Figs 7 and 8 depict the time trajectories of the sliding surfaces of the quadrotor's position and attitude, which converge in finite time to their target trajectories. The total thrust and control torques (e.g. rolling, pitching, and yawing torques) are shown in Fig 9, demonstrating the chattering free of replies. The signal inputs provided by the proposed controller are smooth and have appropriate amplitudes, as shown in Fig 9. The quadrotor follows the intended trajectory, as shown in Fig 11. Fig 10 shows trajectory of output on *xOy* plane. Finally, the results show that, when compared to the ST-PID sliding mode controller, the suggested control method ensures more the quadrotor's stability when subjected to external disturbances.

4.3 Simulation 2

Additional scenario called simulation 2 were carried out to verify the proposed controller's robustness against disturbances. To simulate the external disturbances, we inject a time-

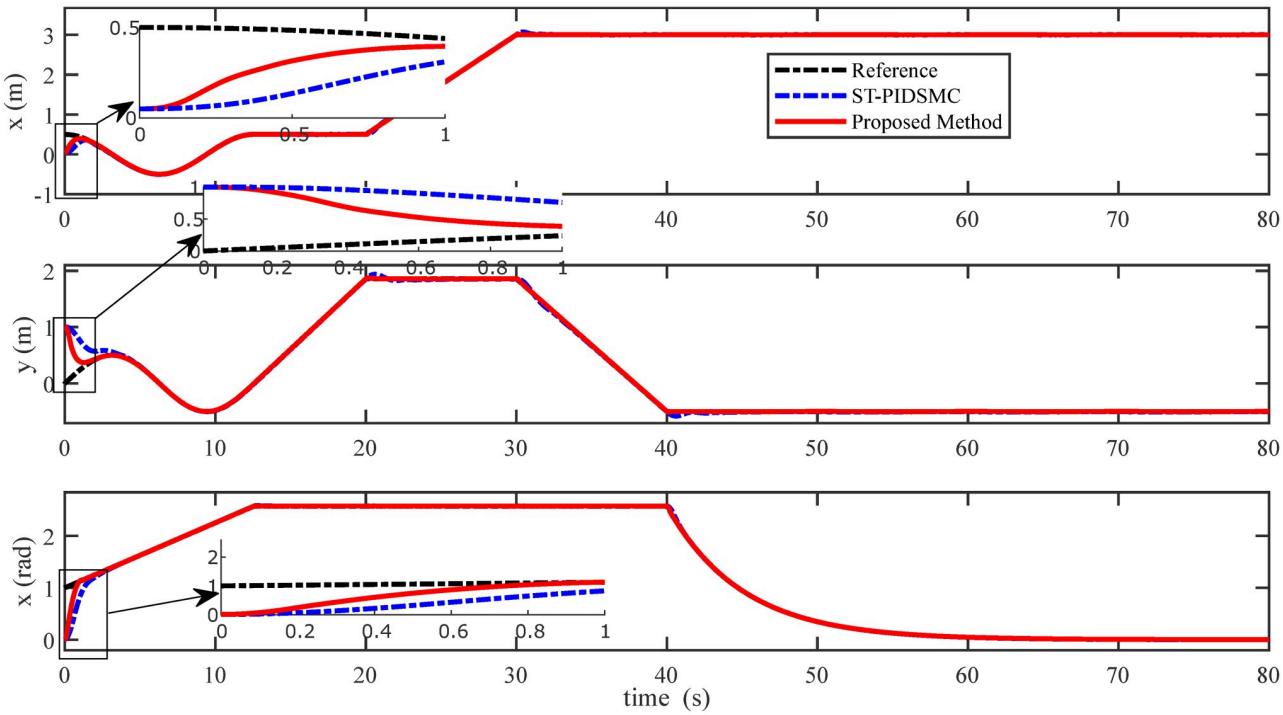

Fig 5. Results of the position under the proposed and ST-PID-SM controllers.

https://doi.org/10.1371/journal.pone.0283195.g005

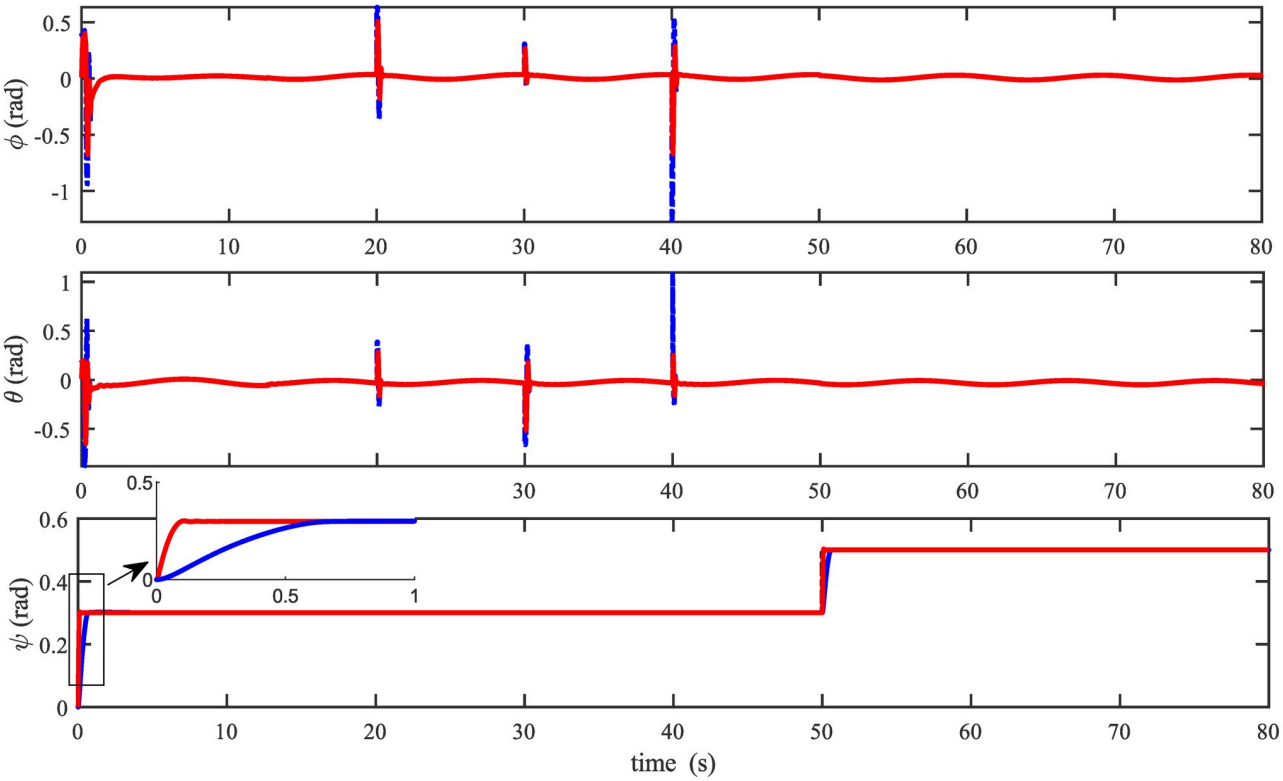

Fig 6. Results of the attitude under the proposed and ST-PID-SM controllers.

https://doi.org/10.1371/journal.pone.0283195.g006

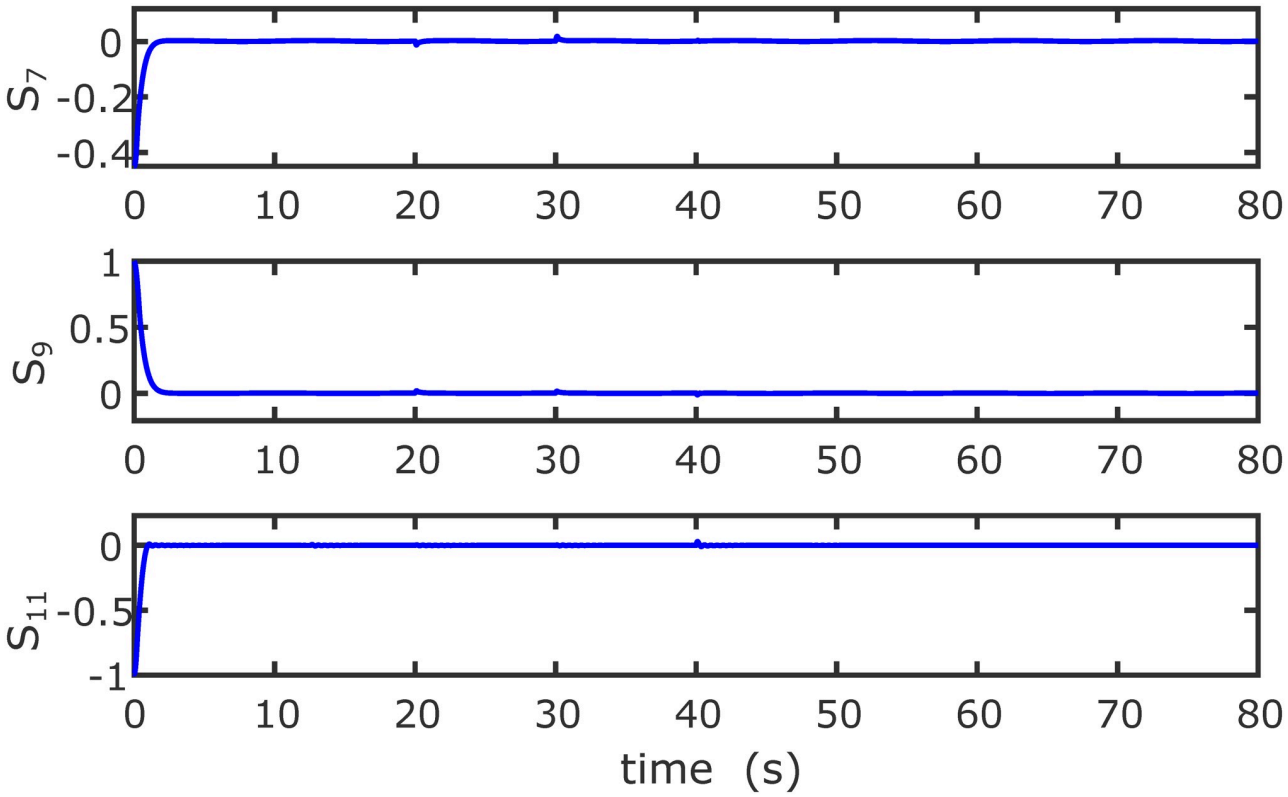

Fig 7. Results of the position sliding variables under the proposed controller.

https://doi.org/10.1371/journal.pone.0283195.g007

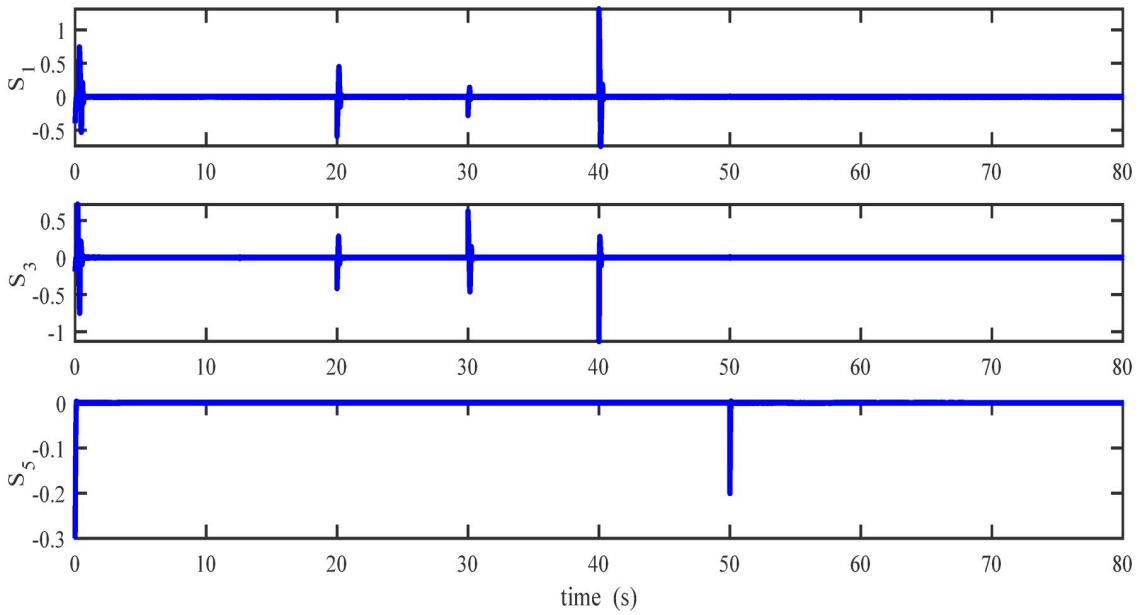

Fig 8. Results of the attitude sliding variables under the proposed controller.

https://doi.org/10.1371/journal.pone.0283195.g008

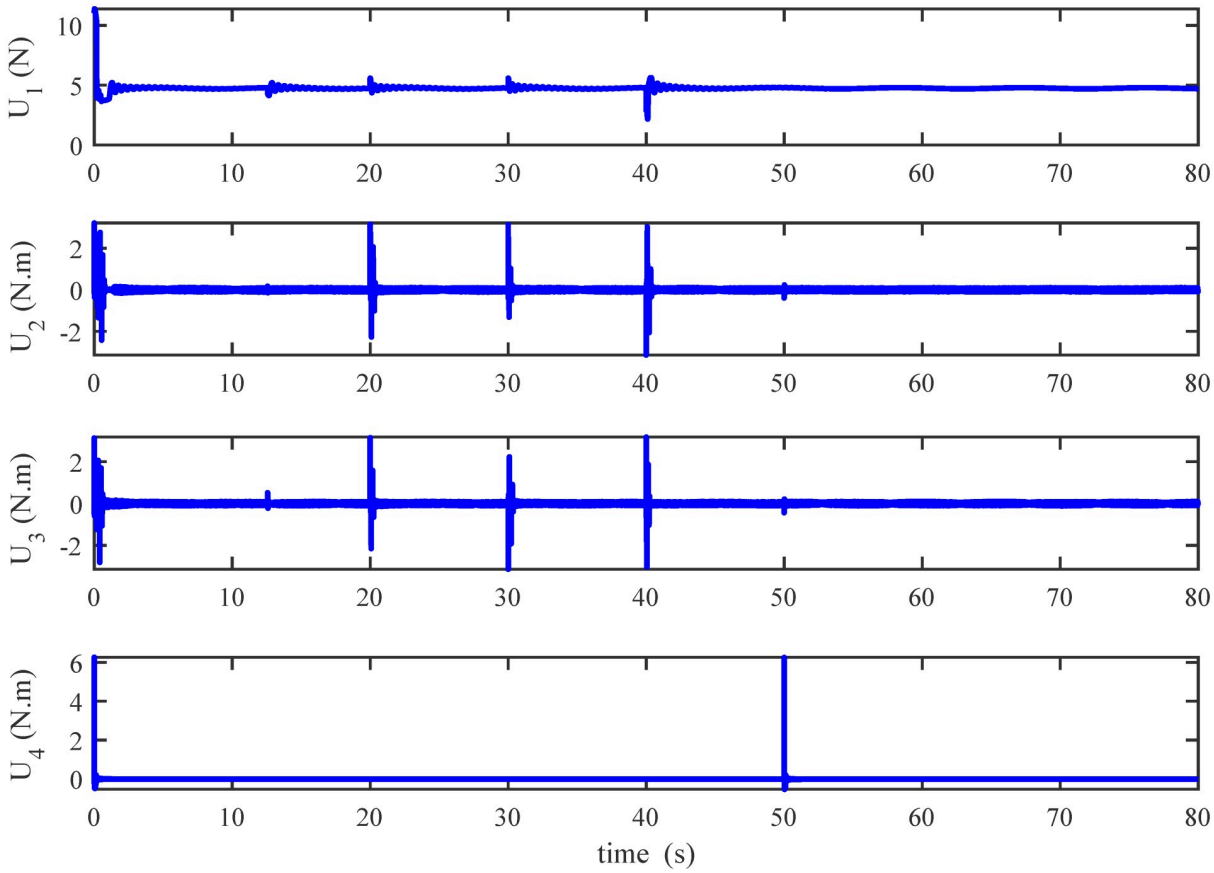

Fig 9. Results of the inputs under the proposed controller.

https://doi.org/10.1371/journal.pone.0283195.g009

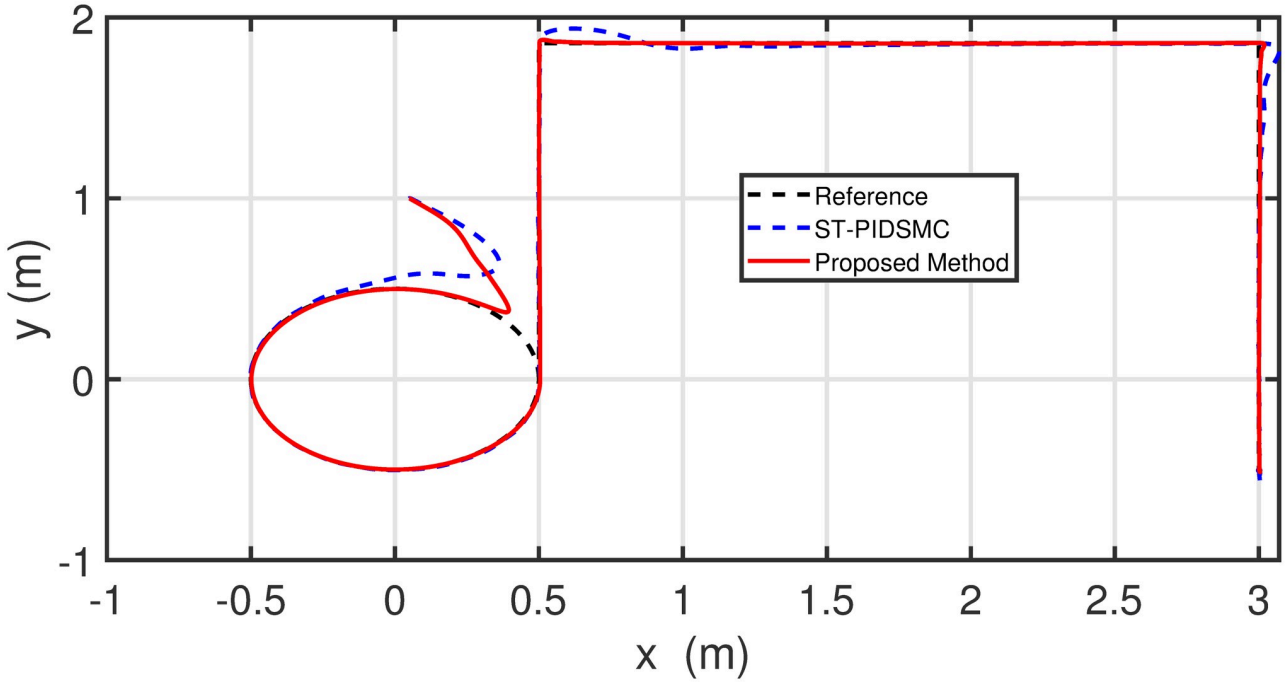

Fig 10. Results of the path following in 2D space under the proposed controller.

https://doi.org/10.1371/journal.pone.0283195.g010

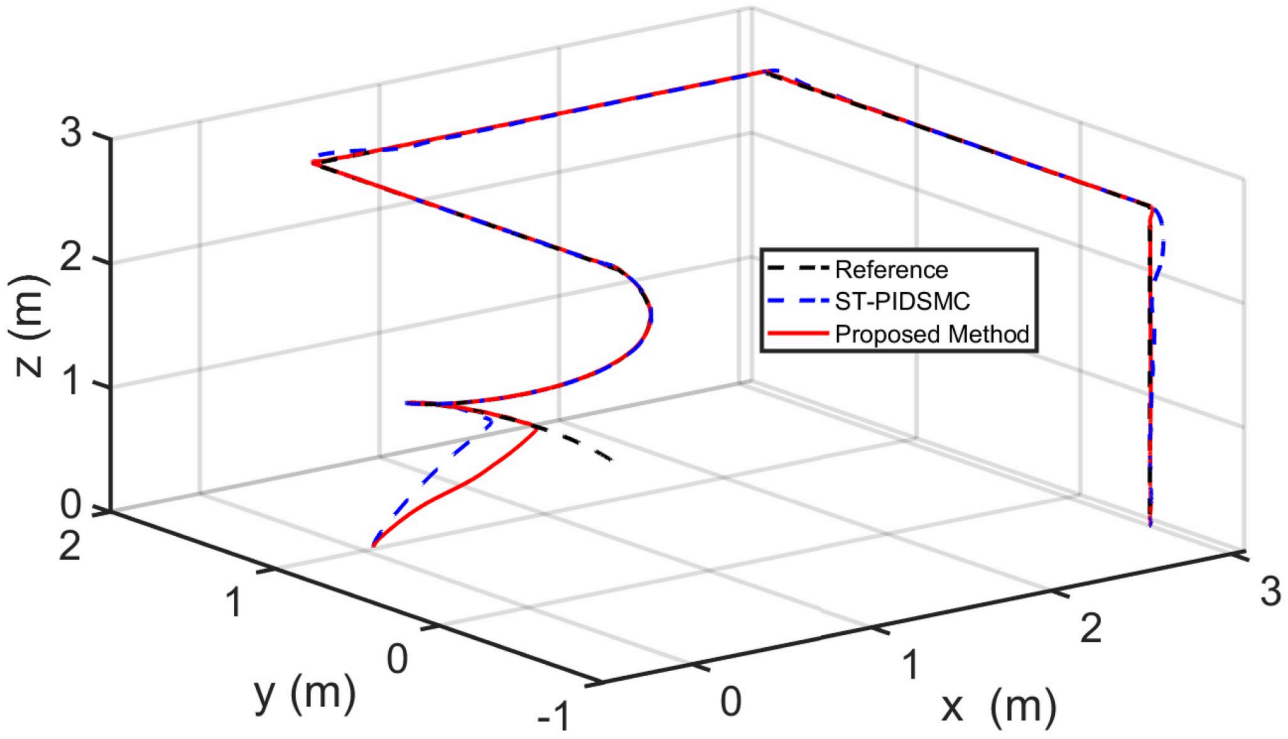

Fig 11. Results of the path following in 3D space under the proposed controller.

https://doi.org/10.1371/journal.pone.0283195.g011

varying disturbance into the model of a quadrotor, as presented in the following equations.

$$\begin{aligned}
\mathcal{D}_x(t) &= 0.5\sin(t) \quad m/s^2 \\
\mathcal{D}_y(t) &= 0.1\cos(t) \quad m/s^2 \\
\mathcal{D}_z(t) &= 0.5\sin(t)\cos(t) \quad m/s^2 \\
\mathcal{D}_\phi(t) &= 0.5\cos(0.5t) \quad rad/s^2 \\
\mathcal{D}_\theta(t) &= 0.5\sin(0.5t) \quad rad/s^2 \\
\mathcal{D}_\psi(t) &= 0.5\sin(0.7t)\cos(0.7t) \quad rad/s^2
\end{aligned} \tag{44}$$

The drag coefficients are supposed to change in the form of Band-Limited White Noise in a limited interval in this simulation. Obviously, the shifting curves of drag coefficients in a real fly in an environment are not more intricate than the ones presented in Figs 12 and 13.

The initial conditions of quadrotor outputs in this case are zero. It should be emphasized that in this simulation,for all flight periods, the external disturbances were applied to the dynamic system to see if the proposed controller could reject the external disturbance and settle down. The outputs of a quadrotor are commended for tracking the following desired trajectory. The results tracking profiles in this simulation under the disturbances are shown in Figs 14–20. It is clear that the proposed control scheme can effectively resist external disturbances and achieve steady-state behavior. Despite this external disturbance, the hyperplane-based sliding mode control strategy provides good responses. The performance of both controllers is assessed by computing their tracking performance in 3D and 2D spaces, which are presented respectively in Figs 19 and 20, in order to clearly show the benefit.Compared to the ST-PID-SMC, the suggested controller significantly reduces the tracking error caused by

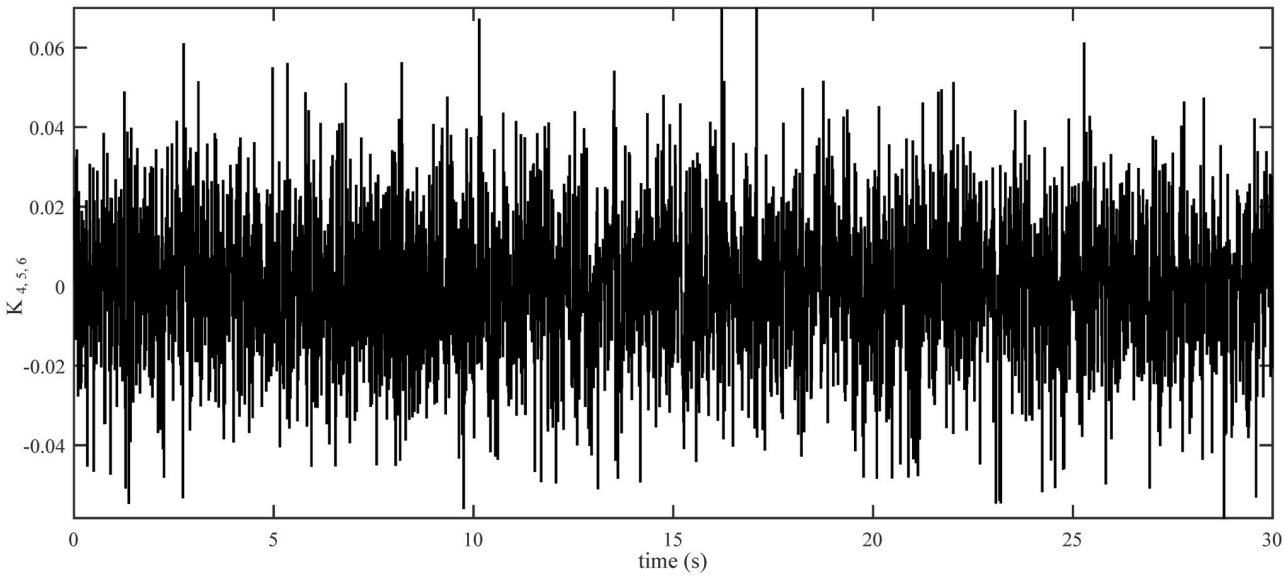

Fig 12. Drag coefficients for translational motion.

https://doi.org/10.1371/journal.pone.0283195.g012

external disturbances. Furthermore, the suggested controller's control signals are substantial and have smaller values (see Fig 18). On the other hand, as shown in Figs 16 and 17, the sliding variables converge to zero in short finite-time. As a result, the suggested control method proposed in this paper for a disturbed quadrotor system has a high level of robustness against time-varying disturbances compared to the results provided by the Ref. [17].

Remark 2. *The dynamic model involves forces and torques applied to the quadcopter as the control actions, in order to achieve the desired reference while taking into account the inertial*

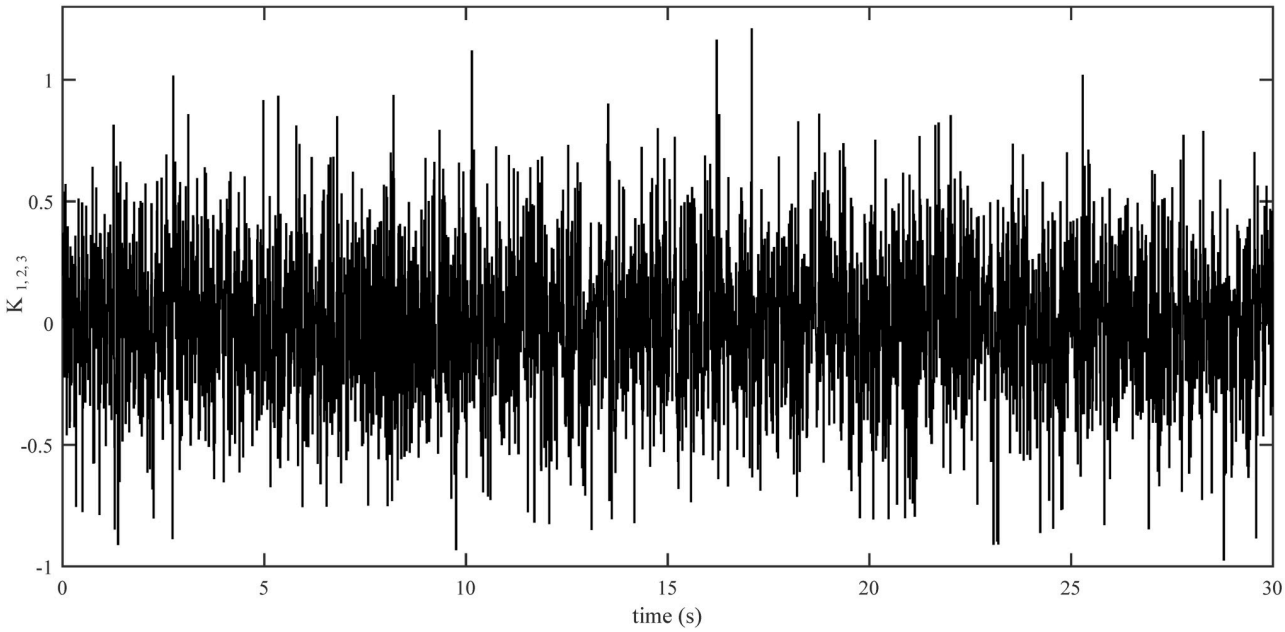

Fig 13. Drag coefficients for rotational motion.

https://doi.org/10.1371/journal.pone.0283195.g013

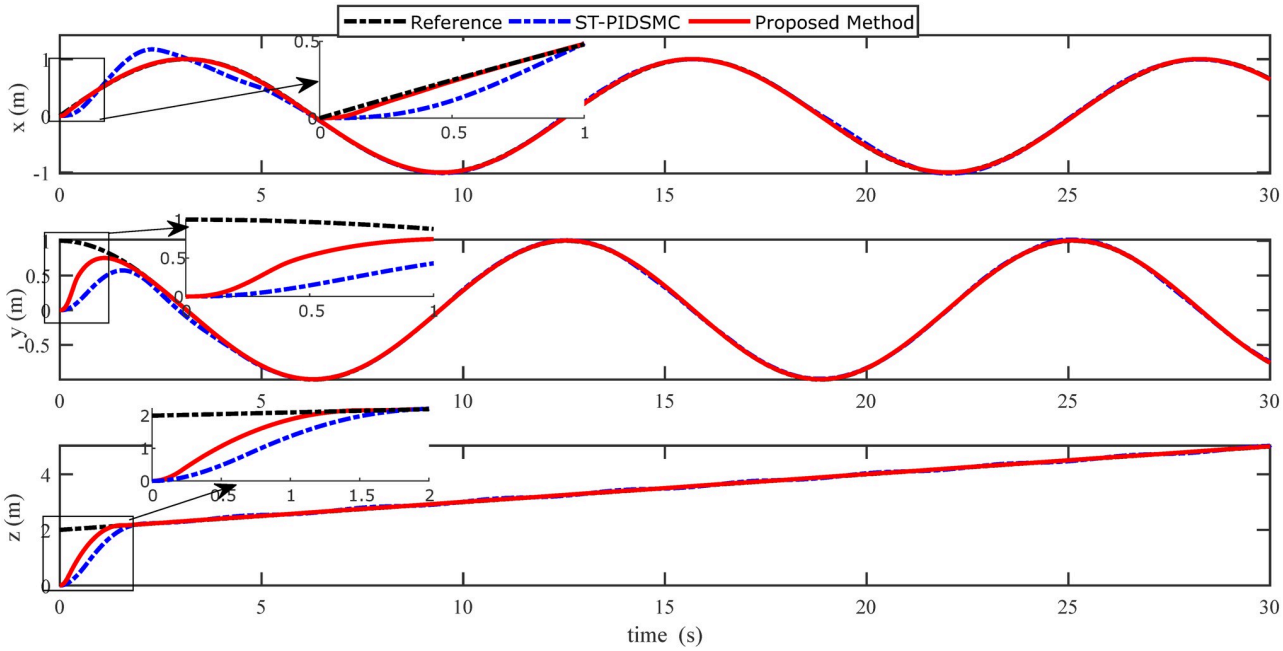

Fig 14. Results of the position under the proposed and ST-PID-SM controllers.

https://doi.org/10.1371/journal.pone.0283195.g014

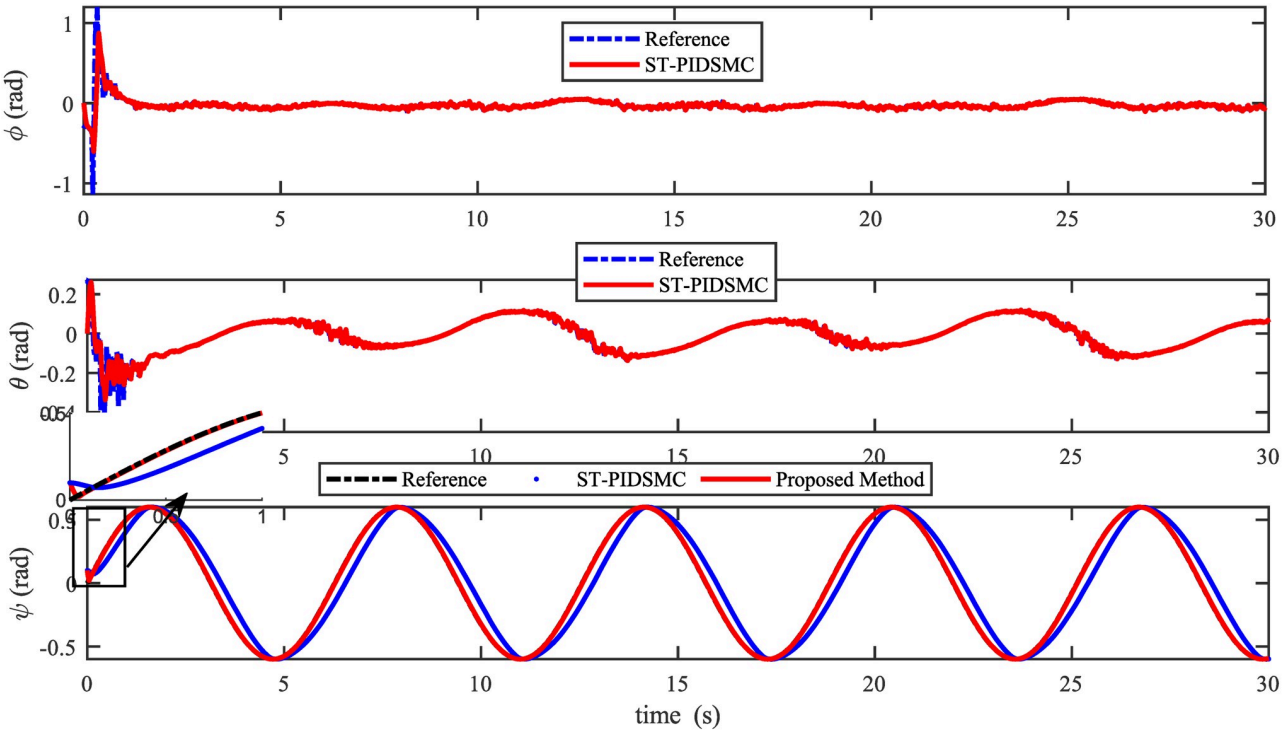

Fig 15. Results of the attitude under the proposed and ST-PID-SM controllers.

https://doi.org/10.1371/journal.pone.0283195.g015

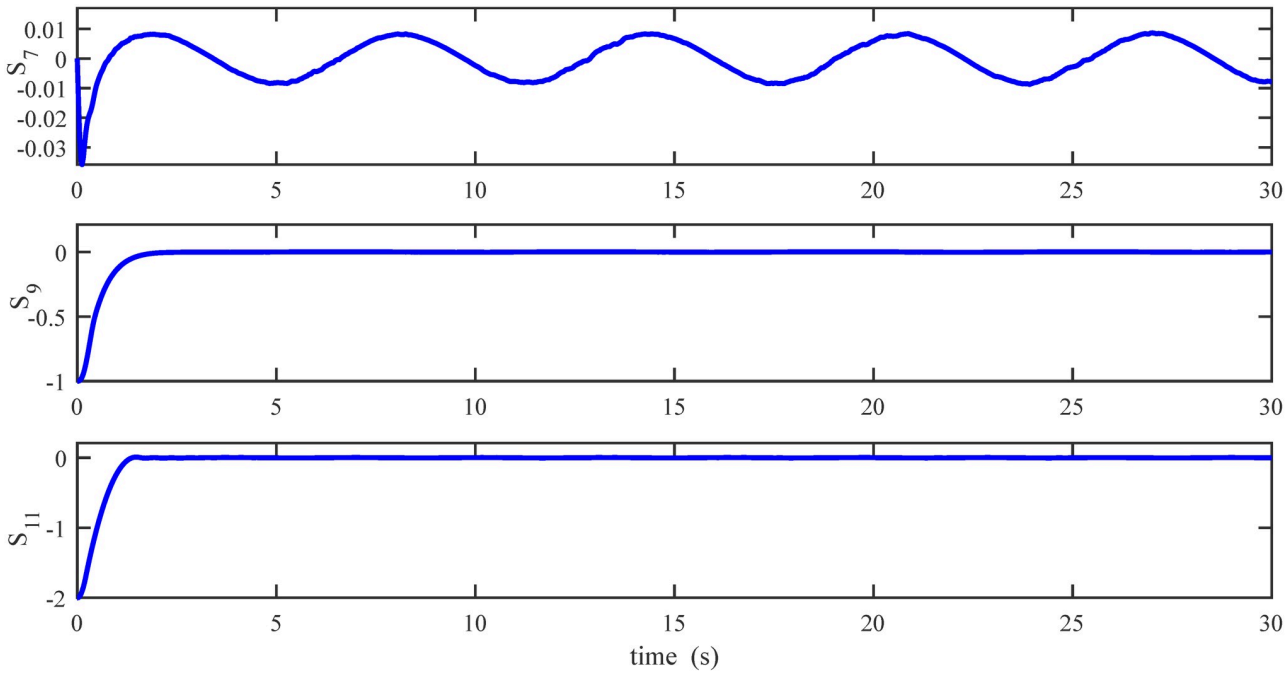

Fig 16. Results of the position sliding variables under the proposed controller.

https://doi.org/10.1371/journal.pone.0283195.g016

properties of the quadcopter. The propulsion control system, together with the servomotors that move various elements, such as the flaps of fixed-wing drones or the swashplate of helicopters, constitute the low-level control. The low-level dynamics, formulated using a first order transfer function of the system, then the dynamics of this part are very fast compared to the quadcopter dynamics. In this research, complex random parametric uncertainties and external disturbances are taken into account in two scenarios in order to make the simulation more realistic.

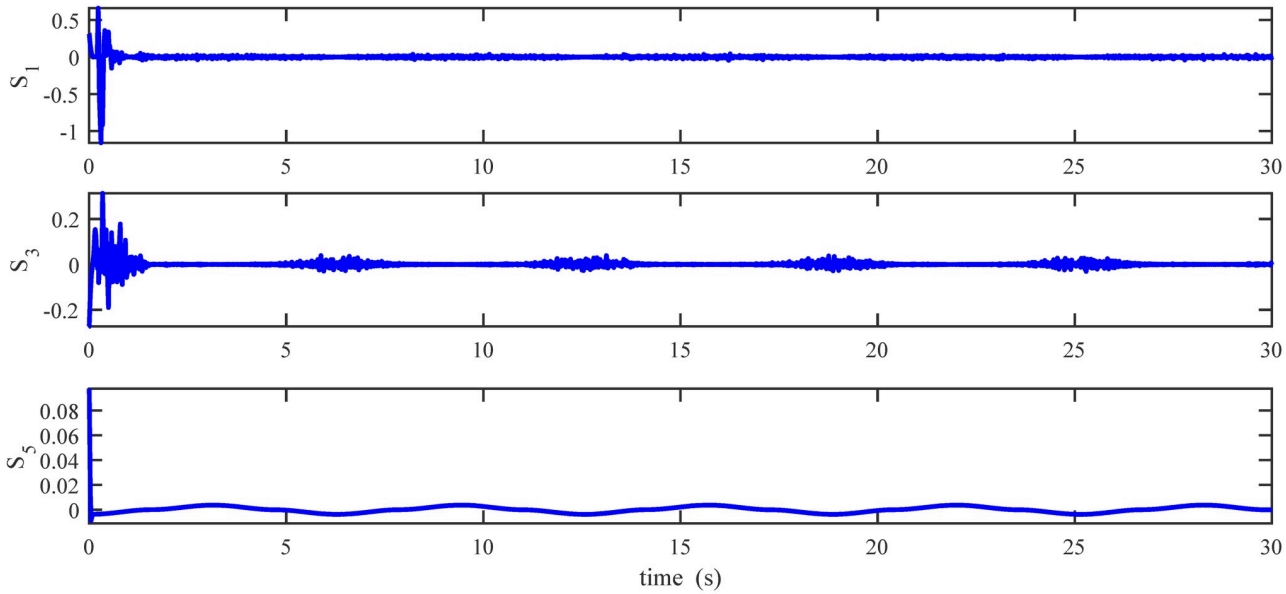

Fig 17. Results of the attitude sliding variables under the proposed controller.

https://doi.org/10.1371/journal.pone.0283195.g017

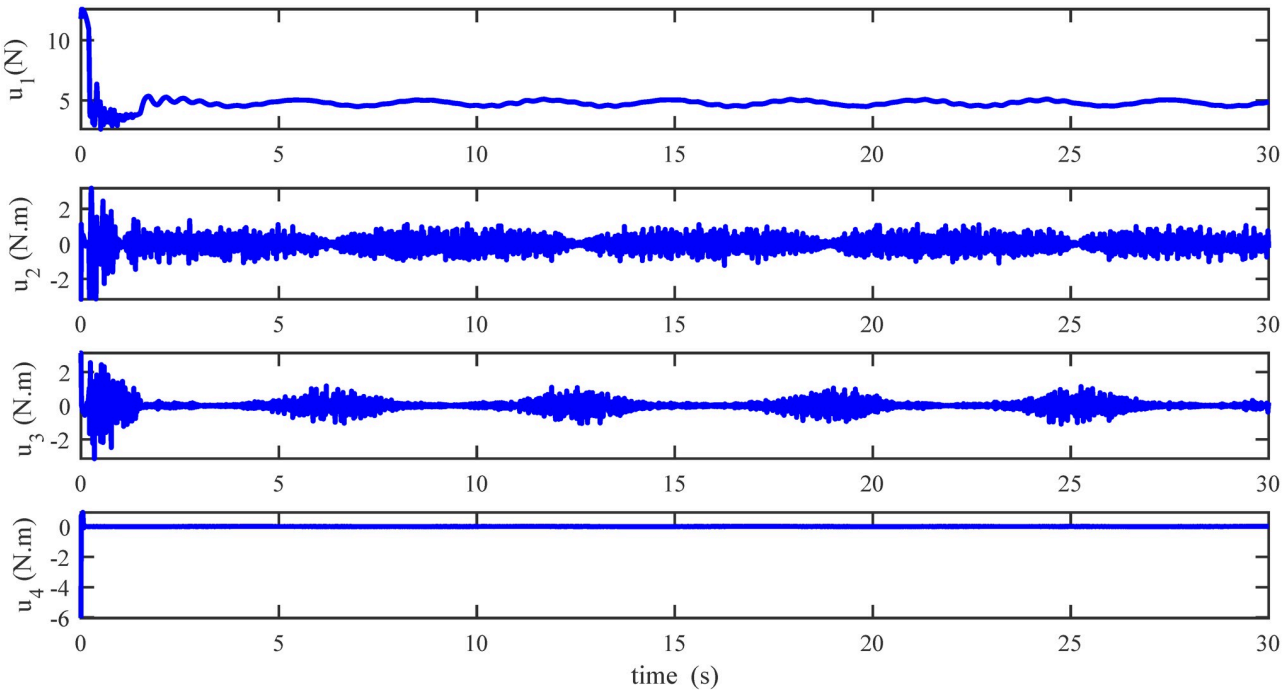

Fig 18. Results of the inputs under the proposed controller.

https://doi.org/10.1371/journal.pone.0283195.g018

4.4 Quantitative analysis of the controllers

The integral of the error square (ISE) and integral absolute error (IAE) are used for quantitative comparison. The ISE and IAE are numerical representations of tracking-error performance.

The ISE and IAE performances of two controllers for the scenario 1 is shown in Tables 3 and 4. Also, Tables 5 and 6 show the ISE and IAE performances for the scenario 2. In comparison to ST-PID-SMC, the finite-time control shows that the ISE and IAE indices are less important for both scenarios.

The superior tracking control performance of the proposed finite-time method is confirmed. It provides more accurate tracking, a faster convergence rate, and excellent robustness than ST-PID-SMC technique.

Compared to the results of the other approaches, the ISE and IAE values for the tracking errors are lower. All of these findings show that the proposed control method achieves better tracking performance, including high precision tracking, quick response, smooth control commands, and high robustness.

Remark 3. *The proposed control method has been compared to ST-PID-SMC technique, which deals with the tracking problem of the quadrotor system subject to external disturbances and parametric uncertainties. Also, in contrast to ST-PID-SMC, where the tracking errors can only asymptotically converge, the proposed control scheme, using a terminal sliding surface manifold, can guarantee the system's finite-time zero-error stability, resulting in better steady-state performance.*

Remark 4. *This note goes at describing the procedure for experimental validation of the finite-time control scheme. In this context, to build the quadrotor test bench experimental to validate the proposed scenarios, a list of the pieces of equipment has been compiled. The hardware configuration of the quadrotor experimental platform is depicted in Fig 21. This platform uses a quadrotor of version X450 with one ground control station, DSP TMS320F28379D, Inertial*

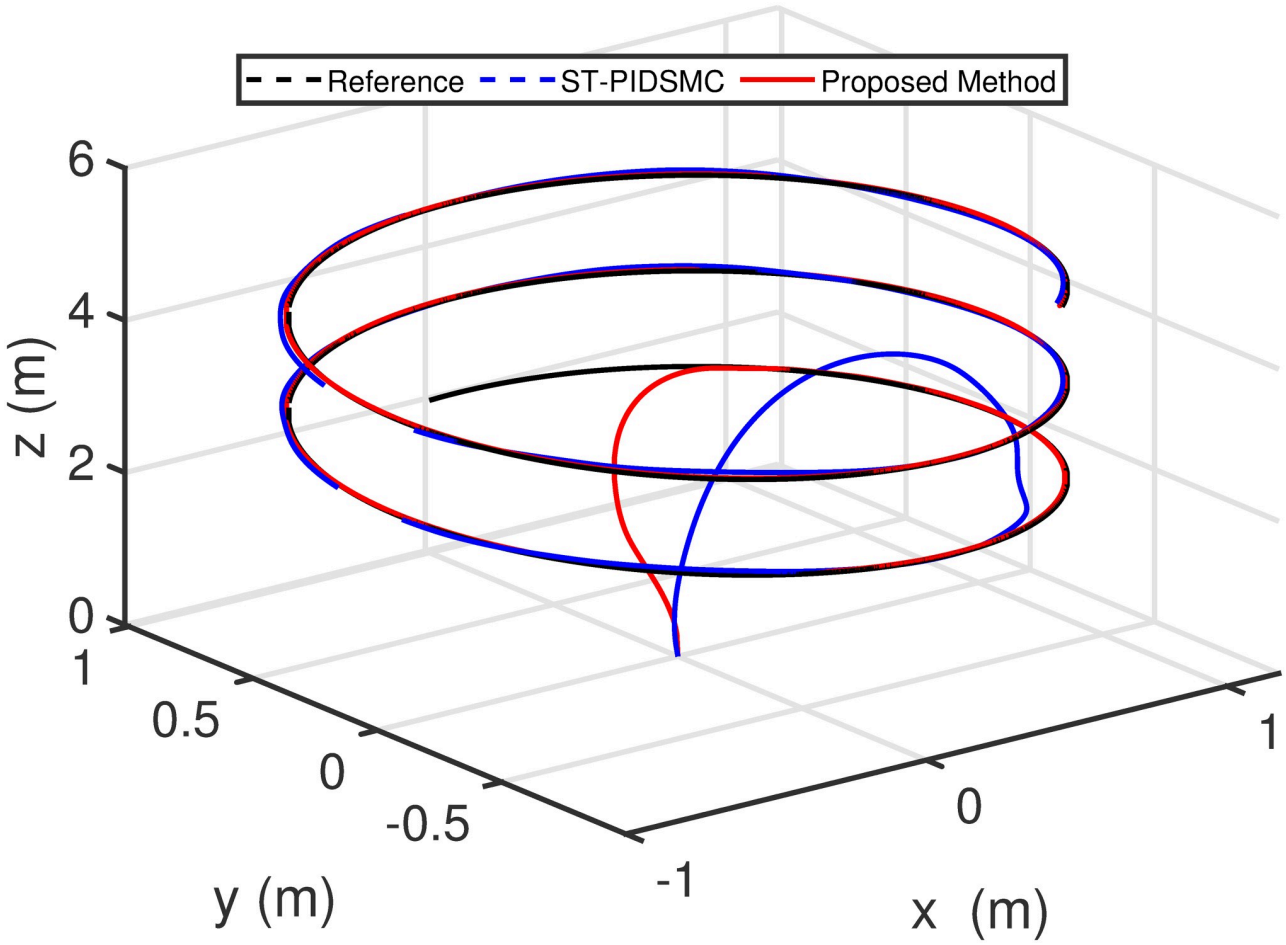

Fig 19. Results of the path following in 2D space under the proposed controller.

https://doi.org/10.1371/journal.pone.0283195.g019

Measurement Unit, the global positioning system module measures the velocity and position in the horizontal plane, and barometric sensor measure the altitude. Moreover, two Zigbee wireless modules ensure the communication between the quadrotor and the ground station. A fan generates the wind then applied as disturbances to the quadrotor.

Remark 5. *The present work presents a finite-time controller for a quadrotor under disturbances using a hyper-plan sliding mode manifold. Also, a switching finite-time is proposed for the system to ensure finite-time stability and cope with the upper bound of the disturbances. Moreover, in the next step, we design the proposed control method's observer or adaptive version.*

5 Conclusions

This paper was devoted to the path following a quadrotor system subject to external disturbances. To begin, the new sliding manifolds for quadrotor attitude and position incorporate two variables of nonlinear sliding surfaces: nonsingular terminal sliding mode and integral terminal sliding mode. The developed sliding manifolds ensured a faster rate of quadrotor state convergence. Second, the switching control laws are built to deal with the most severe wind disturbances. The Lyapunov theory was used to verify the finite-time stability of the proposed control strategy, which improved the tracking performance of a quadrotor control system against wind disturbances. In comparison to supper-twisting PID sliding mode controller, the

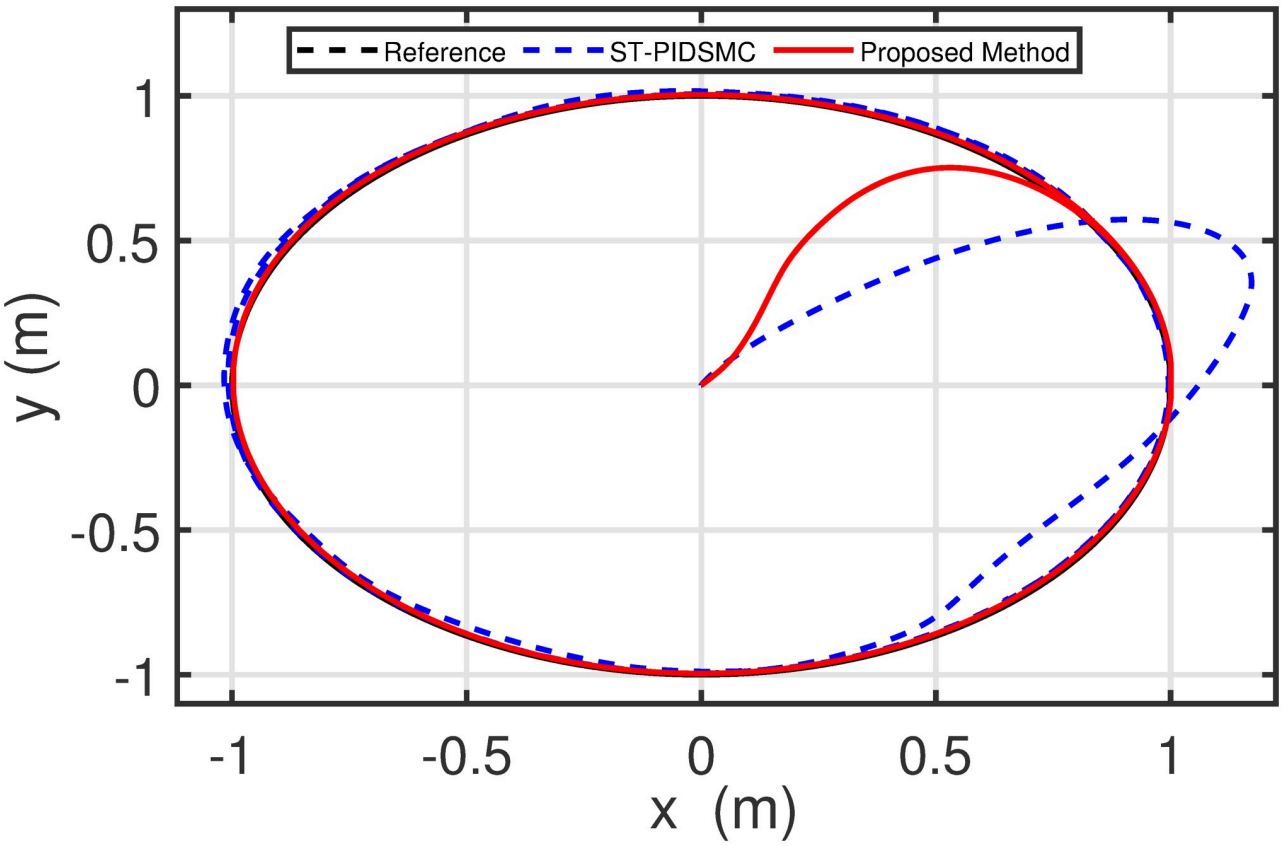

Fig 20. Results of the path following in 3D space under the proposed controller.

https://doi.org/10.1371/journal.pone.0283195.g020

results obtained and the Table 1 show that the control approach suggested in this work has good tracking accuracy, convergence rate, and resilience against wind disturbances.

For further work, the finite-time approach will be validated by experiment. Design a fractional-order finite-time control technique to improve the performances of the proposed

Table 3. ISE performance indexes of the scenario 1.

Variable	Proposed method	ST-PID-SMC
$x(t)$	0.0614	0.1249
$y(t)$	0.3665	0.781
$z(t)$	0.2703	0.5739
$\psi(t)$	0.0028	0.0225

https://doi.org/10.1371/journal.pone.0283195.t003

Table 4. IAE performance indexes of the scenario 1.

Variable	Proposed method	ST-PID-SMC
$x(t)$	0.3979	0.6126
$y(t)$	0.6902	1.87
$z(t)$	0.5382	1.017
$\psi(t)$	0.0295	0.1349

https://doi.org/10.1371/journal.pone.0283195.t004

Table 5. ISE performance indexes of the scenario 2.

Variable	Proposed method	ST-PID-SMC
$x(t)$	0.0012	0.13
$y(t)$	0.358	0.72
$z(t)$	1.46	2.53
$\psi(t)$	0.0002	0.323

https://doi.org/10.1371/journal.pone.0283195.t005

Table 6. IAE performance indexes of the scenario 2.

Variable	Proposed method	ST-PID-SMC
$x(t)$	0.164	1.164
$y(t)$	0.63	1.35
$z(t)$	1.22	2.34
$\psi(t)$	0.0581	2.66

https://doi.org/10.1371/journal.pone.0283195.t006

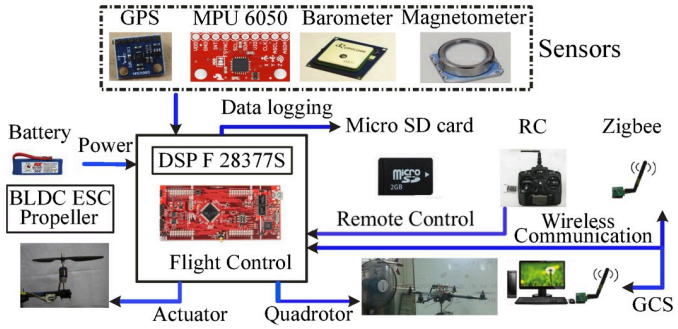

Fig 21. The quadrotor's hardware structure.

https://doi.org/10.1371/journal.pone.0283195.g021

control method. Also, the fault-tolerant control problem of the quadrotor actuators and sensors will be addressed using the adaptive version of the proposed finite-time controller. Innovative solutions and sensors have recently been created for civilian use, thanks to new technologies, allowing for more flexibility (fewer restrictions in terms of sensor installation), performance (longer duration, better aerodynamic profile, better navigation system), and planning tools. The development of low-cost flight controller systems and the widespread dissemination of structure from motion applications, which allow the production of a 3D model from a sequence of photos collected from various points of view, are the most recent advancements in quadrotor aircrafts.

Author Contributions

Conceptualization: Jamshed Iqbal.

Data curation: Moussa Labbadi.

Formal analysis: Moussa Labbadi.

Investigation: Moussa Labbadi, Mohamed Djemai.

Methodology: Moussa Labbadi, Mohamed Djemai, Yassine Boukal, Yassine Bouteraa.

Project administration: Mohamed Djemai.

Resources: Jamshed Iqbal.

Software: Yassine Boukal, Yassine Bouteraa.

Supervision: Jamshed Iqbal.

Validation: Jamshed Iqbal.

Visualization: Yassine Bouteraa.

Writing – original draft: Moussa Labbadi, Yassine Boukal.

Writing – review & editing: Jamshed Iqbal.

References

1. Mairaj A., Baba A. I., and Javaid A. Y., Application specific drone simulators: Recent advances and challenges, Simulation Modelling Practice and Theory, vol. 94, pp. 100–117, Jul. 2019. https://doi.org/10.1016/j.simpat.2019.01.004
2. Hassanalian M. and Abdelkefi A., Classifications, applications, and design challenges of drones: A review, Progress in Aerospace Sciences, vol. 91, pp. 99–131, May 2017. https://doi.org/10.1016/j.paerosci.2017.04.003
3. Anjum M., Khan Q., Ullah S., Hafeez G., Fida A., Iqbal J., et al., Maximum power extraction from a standalone photo voltaic system via neuro-adaptive arbitrary order sliding mode control strategy with high gain differentiation, Applied Sciences, 12(6): 2773, 2022 https://doi.org/10.3390/app12062773
4. Ullah S., Mehmood A., Khan Q., Rehman S. and Iqbal J., Robust integral sliding mode control design for stability enhancement of underactuated quadcopter, International Journal of Control, Automation and Systems, 18(7):1671–1678, 2020 https://doi.org/10.1007/s12555-019-0302-3
5. T.-W. Ou and Y.-C. Liu, Adaptive Backstepping Tracking Control for Quadrotor Aerial Robots Subject to Uncertain Dynamics, 2019 American Control Conference (ACC), Jul. 2019.
6. A. Benaddy, M. Labbadi, and M. Bouzi, Adaptive Nonlinear Controller for the Trajectory Tracking of the Quadrotor with Uncertainties, 2020 2nd Global Power, Energy and Communication Conference (GPECOM), Oct. 2020.
7. M. Labbadi, Y. Boukal, M. Taleb, and M. Cherkaoui, Fractional order sliding mode control for the tracking problem of Quadrotor UAV under external disturbances, 2020 European Control Conference (ECC), May 2020.
8. Hua C., Chen J., and Guan X., Fractional-order sliding mode control of uncertain QUAVs with time-varying state constraints, Nonlinear Dyn., 2018.
9. Shi X., Cheng Y., Yin C., Dadras S., and Huang X., Design of Fractional-Order Backstepping Sliding Mode Control for Quadrotor UAV, Asian J. Control.
10. Vahdanipour M. and Khodabandeh M., Adaptive Fractional Order Sliding Mode Control for a Quadrotor with a Varying Load, Aerosp. Sci. Technol., vol. 86, pp. 737747, 2019. https://doi.org/10.1016/j.ast.2019.01.053
11. Wang J., Ma X., Li H., and Tian B., Self-triggered sliding mode control for distributed formation of multiple quadrotors, Journal of the Franklin Institute, vol. 357, no. 17, pp. 12223–12240, Nov. 2020. https://doi.org/10.1016/j.jfranklin.2020.09.008
12. Labbadi M. and Cherkaoui M., Robust adaptive backstepping fast terminal sliding mode controller for uncertain quadrotor UAV, Aerospace Science and Technology, vol. 93, p. 105306, Oct. 2019. https://doi.org/10.1016/j.ast.2019.105306
13. Labbadi M., El H. Moussaoui, An improved adaptive fractional-order fast integral terminal sliding mode control for distributed quadrotor, Math. Comput. Simul. 188 (2021) 120–134. https://doi.org/10.1016/j.matcom.2021.03.039
14. Zatout M. S., Rezoug A., Rezoug A., Baizid K. and Iqbal J., Optimization of fuzzy logic quadrotor attitude controller—Particle swarm, Cuckoo search and BAT algorithms, International Journal of Systems Science, 2021. https://doi.org/10.1080/00207721.2021.1978012
15. Labbadi M. and Cherkaoui M., Robust adaptive nonsingular fast terminal sliding-mode tracking control for an uncertain quadrotor UAV subjected to disturbances, ISA Transactions, vol. 99, pp. 290–304, Apr. 2020. https://doi.org/10.1016/j.isatra.2019.10.012 PMID: 31703850

16. Khan O., Pervaiz M., Ahmad E. and Iqbal J., On the derivation of novel model and sophisticated control of flexible joint manipulator, Revue Roumaine des Sciences Techniques-Serie Electrotechnique et Energetique, 62(1): 103–108, 2017

17. Labbadi M. and Cherkaoui M., Novel robust super twisting integral sliding mode controller for a quadrotor under external disturbances, International Journal of Dynamics and Control, vol. 8, no. 3, pp. 805–815, Dec. 2019. https://doi.org/10.1007/s40435-019-00599-6

18. Singh P., Gupta S., Behera L., Verma N. K., and Nahavandi S., Perching of Nano-Quadrotor Using Self-Trigger Finite-Time Second-Order Continuous Control, IEEE Systems Journal, pp. 1–11, 2020.

19. Goel A. and Mobayen S., Adaptive nonsingular proportional-integral-derivative-type terminal sliding mode tracker based on rapid reaching law for nonlinear systems, Journal of Vibration and Control, p. 107754632096428, Sep. 2020.

20. Kidambi K. B., Fermüller C., Aloimonos Y. and Xu H., Robust Nonlinear Control-Based Trajectory Tracking for Quadrotors Under Uncertainty, in IEEE Control Systems Letters, vol. 5, no. 6, pp. 2042–2047, Dec. 2021. https://doi.org/10.1109/LCSYS.2020.3044833

21. Dou L., Su X., Zhao X., Zong Q., and He L., Robust tracking control of quadrotor via onpolicy adaptive dynamic programming, International Journal of Robust and Nonlinear Control, vol. 31, no. 7, pp. 2509–2525, Feb. 2021. https://doi.org/10.1002/rnc.5419

22. Ghadiri H., Emami M., Khodadadi H., Adaptive super-twisting non-singular terminal sliding mode control for tracking of quadrotor with bounded disturbances, Aerosp. Sci. Technol. 112 (2021) 106616. https://doi.org/10.1016/j.ast.2021.106616

23. Liu K., Wang R., Wang X., Wang X., Anti-saturation adaptive finite-time neural network based fault-tolerant tracking control for a quadrotor UAV with external disturbances, Aerosp. Sci. Technol. 115 (2021) 106790. https://doi.org/10.1016/j.ast.2021.106790

24. Ma D., Xia Y., Shen G., Jiang H., Hao C., Practical Fixed-time Disturbance Rejection Control for Quadrotor Attitude Tracking, IEEE Trans. Ind. Electron. 0046 (2020) 1–1. https://doi.org/10.1109/tie.2020.3001800

25. Mechali O., Xu L., Huang Y., Shi M., Xie X., Observer-based fixed-time continuous nonsingular terminal sliding mode control of quadrotor aircraft under uncertainties and disturbances for robust trajectory tracking: Theory and experiment, Control Eng. Pract. 111 (2021) 104806. https://doi.org/10.1016/j.conengprac.2021.104806

26. Nekoukar V., Mahdian N. Dehkordi, Robust path tracking of a quadrotor using adaptive fuzzy terminal sliding mode control, Control Eng. Pract. 110 (2021) 104763. https://doi.org/10.1016/j.conengprac.2021.104763

27. Oliva-Palomo F., Sanchez-Orta A., Alazki H., Castillo P., Muñoz-Vázquez A.J., Robust global observer position-yaw control based on ellipsoid method for quadrotors, Mech. Syst. Signal Process. 158 (2021). https://doi.org/10.1016/j.ymssp.2021.107721

28. Wu X., Zheng W., Zhou X., Shao S., Adaptive dynamic surface and sliding mode tracking control for uncertain QUAV with time-varying load and appointed-time prescribed performance, J. Franklin Inst. 358 (2021) 4178–4208. https://doi.org/10.1016/j.jfranklin.2021.03.018

29. Yue X., Shao X., Li J., Prescribed chattering reduction control for quadrotors using aperiodic signal updating, Appl. Math. Comput. 405 (2021) 126264. https://doi.org/10.1016/j.amc.2021.126264

30. Mofid O. and Mobayen S., Adaptive Finite-Time Backstepping Global Sliding Mode Tracker of Quad-Rotor UAVs Under Model Uncertainty, Wind Perturbation, and Input Saturation, in IEEE Transactions on Aerospace and Electronic Systems, vol. 58, no. 1, pp. 140–151, Feb. 2022. https://doi.org/10.1109/TAES.2021.3098168

31. Alattas K.A., Mofid O., Alanazi A.K., Abodief H.M., Bartoszewicz A., Bakouri M., et al, Barrier Function Adaptive Nonsingular Terminal Sliding Mode Control Approach for Quad-Rotor Unmanned Aerial Vehicles, Sensors. 22 (2022). https://doi.org/10.3390/s22030909 PMID: 35161656

32. Díaz-Méndez Y, de Jesus LD, de Sousa MS, Cunha SS, Ramos AB. Conditional integrator sliding mode control of an unmanned quadrotor helicopter. Proceedings of the Institution of Mechanical Engineers, Part I: Journal of Systems and Control Engineering. 2022; 236(3):458–472. https://doi.org/10.1177/09596518211049861

33. Dalwadi N., Deb D., Muyeen S.M., Observer based rotor failure compensation for biplane quadrotor with slung load, Ain Shams Eng. J. 13 (2022) 101748. https://doi.org/10.1016/j.asej.2022.101748

34. Dalwadi N., Deb D., Rath J.J., Biplane Trajectory Tracking Using Hybrid Controller Based on Backstepping and Integral Terminal Sliding Mode Control, Drones. 6 (2022) 1–16. https://doi.org/10.3390/drones6030058

35. Dalwadi N., Deb D., Kothari M., Ozana S., Disturbance observer-based backstepping control of tail-sitter uavs, Actuators. 10 (2021) 1–24. https://doi.org/10.3390/act10060119

36. Xu Q., Continuous integral terminal third-order sliding mode motion control for piezoelectric nanopositioning system, IEEE/ASME Trans. Mechatron., vol. 22, no. 4, pp. 1828–1838, Aug. 2017. https://doi.org/10.1109/TMECH.2017.2701417

37. Feng Y., Yu X., Man Z.: Non-singular terminal sliding mode control of rigid manipulators, Automatica, 2002, 38, (12), pp. 2159–2167. https://doi.org/10.1016/S0005-1098(02)00147-4

38. Khawwaf J., Zheng J., Chai R., Lu R., and Man Z., Adaptive Microtracking Control for an Underwater IPMC Actuator Using New Hyperplane-Based Sliding Mode, IEEE/ASME Transactions on Mechatronics, vol. 24, no. 5, pp. 2108–2117, Oct. 2019. https://doi.org/10.1109/TMECH.2019.2937328

39. Freire F. P., Martins N. A., and Splendor F., A Simple Optimization Method for Tuning the Gains of PID Controllers for the Autopilot of Cessna 182 Aircraft Using Model-in-the-Loop Platform, J. Control. Autom. Electr. Syst., vol. 29, no. 4, pp. 441–450, 2018. https://doi.org/10.1007/s40313-018-0391-x